International Journal of Hydrogen Energy 83 (2024) 1003–1023

Contents lists available at ScienceDirect

International Journal of Hydrogen Energy

journal homepage: www.elsevier.com/locate/he

Application of hybrid chaotic particle swarm optimization and slime mould algorithm to optimally estimate the parameter of fuel cell and solar PV system☆

Jyoti Gupta [a], Svetlana Beryozkina [b], Mohammad Aljaidi [c], Manish Kumar Singla [d,e,*], Murodbek Safaraliev [f], Anupma Gupta [d], Parag Nijhawan [g]

[a] School of Engineering and Technology, K.R. Mangalam University, 122103, Sohna Road, Gurugram, Haryana, India
[b] College of Engineering and Technology, American University of the Middle East, Egaila, 54200, Kuwait
[c] Department of Computer Science, Faculty of Information Technology Zarqa University, Zarqa, 13110 Jordan
[d] Department of Interdisciplinary Courses in Engineering, Chitkara University Institute of Engineering and Technology, Chitkara University, Punjab, India
[e] Jadara University Research Center, Jadara University, Jordan
[f] Department of Automated Electrical Systems, Ural Federal University, 620002, Yekaterinburg, Russia
[g] Electrical and Instrumentation Engineering Department, Thapar Institute of Engineering and Technology, Patiala, India

ARTICLE INFO

Keywords:
Hydrogen
Parameter estimation
PV
PEM fuel cell
Mathematical modeling
Optimization
HCPSOSMA
Non-parametric test

ABSTRACT

Through the use of fuel cells and photovoltaic (PV) solar cells, green energy has become one of the most popular developments in electricity generation in recent years. Accurate modeling of fuel cell and PV cell is critical in the simulation and analysis of energy systems that use both sources. Due to the complexity and nonlinearity of these hybrid systems, the model must be optimized under different operating conditions. In this article, a novel metaheuristic efficient hybrid algorithm is proposed for this purpose. A Hybrid Chaotic Particle Swarm Optimization and Slime Mould Algorithm (HCPSOSMA) has been proposed to estimate the PV/fuel cell system parameters. The hybrid HCPSOSMA algorithm is superior to other algorithms in terms of higher accuracy in searching for optimal solutions and better explorative capability. The problem formulation is based on minimizing the Root Mean Square Error (RMSE) between the calculated values and measured values for both the triple-diode PV model and the proton exchange membrane (PEM) fuel cell. The results show that the hybrid algorithm outperforms other algorithms in determining the best PV/PEMFC parameters that produce accurate V–I and P–I characteristic curves and the RMSE is about 4 × 10–12. Finally, non-parametric tests based on Friedman's ranking, Wilcoxon's rank sum test and Kruskal-Wallis test are implemented to prove the superiority of the proposed hybrid algorithm in the parameter estimation.

Nomenclature

Abbreviation	Name
PV	photovoltaic
HCPSOSMA	Hybrid Chaotic Particle Swarm Optimization and Slime Mould Algorithm
RMSE	Root Mean Square Error
PEM	Proton exchange membrane
GOA	Grasshopper optimization algorithm
SSA	Salp Swarm Algorithm
MVO	Multi-Verse Optimizer
GWO	Grey Wolf Optimizer
MPSO	Modified Particle Swarm Optimizer
TLBO-DE	Hybrid Teaching Learning Based Optimization
MPA	Marine Predator Algorithm
HAS	Harmony Search Algorithm
BPSO	Barebones Particle Swarm Optimizer
GAMNU	Genetic Algorithm based on non-uniform mutation

(*continued on next column*)

(*continued*)

(*continued on next page*)

☆ This paper is the English version of the paper reviewed and published in Russian in «International Scientific Journal for Alternative Energy and Ecology». ISJAEE, 423, #06 (2024).

* Corresponding author.
E-mail address: manish.singla@chitkara.edu.in (M.K. Singla).

https://doi.org/10.1016/j.ijhydene.2024.08.048
Received 30 January 2024; Accepted 28 July 2024
0360-3199/© 2024 Hydrogen Energy Publications LLC. Published by Elsevier Ltd. All rights are reserved, including those for text and data mining, AI training, and similar technologies.

(*continued*)

Abbreviation	Name
PSO	Particle Swarm Optimization
CSA	Cuckoo Search Algorithm
CICA	Chaos Induced Coyote Algorithm
ABO	Artificial Bee Colony
BFO	Bacterial Foraging Optimization
LGOA	Levy Flight Based Grasshopper Optimization Algorithm
FPA	Flower Pollination Algorithm
JAYA	Jaya Optimization Algorithm
EOTLBO	Either-Or Teaching Learning Based Algorithm
BMO	Bird Mating Optimization Algorithm
BMO	Nelder-Mead Simplex Algorithm Based On Eagle Startegy
CA	Camel Behavior Search Algorithm
HROA	Hybrid RAO Optimizer
PO	Political Optimizer
FODPSO	Fractional Order Darwinian Particle Swarm Optimization
IEO	Improved Equilibrium Optimizer
ASMA	Adaptive Slime Mould Algorithm
ICA	Imperialist Competitive Algorithm
HS	Harmony Search
FA	Firefly Algorithm
CGBO	Chaotic Gradient-Based Optimization
MFO	Moth-Flame Optimization
WCA	Water Cycle Algorithm
SFL	Shuffled Frog Leaping
SSE	Sum of Square Error
TDM	Triple-Diode Model
SMA	Slime Mould Algorithm
ALO	Ant Lion Optimizer
ASO	Atom Search Optimization
HHO	Harris Hawk Optimization
Symbols	Name
V_{stack}	stack output voltage
N_{cells}	number of cells
V_{cell}	voltage of each cell
$V_{activation}$	activation voltage drop
V_{ohmic}	ohmic voltage drop
$V_{concentration}$	concentration voltage drop
E_{Nernst}	open circuit voltage
T_{fc}	operating cell temperature
P_{O2}	partial pressures of oxygen
P_{H2}	partial pressures of hydrogen
P_a	pressure at the anode
P_c	pressure at the cathode
PH_a	relative vapour humidity around the anode
RH_C	relative vapour humidity around the cathode
I_{fc}	current generated by the cell
A	surface area of the membrane
P_{H2O}	water saturation pressure
ξ_1, ξ_2, ξ_3, ξ_4	semi-empirical coefficients
C_{O2}	oxygen concentration
R_M	membrane surface resistance
R_C	resistance connection
ρM	specific resistance of the membrane material
l	membrane thickness
λ	adjustable empirical variable
b	parametric variable
$Jmax$	maximum current density.
V_{actual}	actual experiment voltage
V_i	calculated model voltage
N	quantity of data points
I	Output cell current
I_{ph}	Photovoltaic current
I_o, I_{o1}, I_{o2}	Saturation current of each diode
q	Electronic charge
V	Output voltage
R_S	Series resistance
$\alpha, \alpha_1, \alpha_2$	Ideality factor of each diode
K	Boltzmann's Constant
T	Cell temperature
R_{Sh}	Shunt resistance
V_{OC}	Open circuit voltage
I_{SC}	Short circuit current
V_{mp}	Voltage at maximum power point
I_{mp}	Current at maximum power point
P	quantity of data points

(*continued on next column*)

(*continued*)

Abbreviation	Name
$f(cp_k^i)$	function that creates a chaotic model
x_{k+1}	Output value at particular iteration
x_k	variable
a	constant

1. Introduction

The keyword "Green Energy Technology" attracts many researchers and experts to produce electricity and fuel from natural resources without emissions. Throughout the nation, stringent environmental regulations and energy subsidies have been implemented to promote the creation and use of renewable energy technologies, such as solar, wind, tidal, fuel cell, and other energy resources, in order to meet the demands of alternative energy generation and environmental sustainability [1]. Among the many strategies for renewable energy generation, fuel cells and solar PV panels have received much attention [2]. Proton exchange membrane (PEM) is among the most popular fuel cells with many desirable properties, such as low noise, low operating temperature, zero emissions, high energy density and improved lifetime [3]. The proton is used for conduction for ion exchange purposes; Thus, a proton exchange membrane fuel cell is often referred to as a polymer electrolyte membrane fuel cell [4]. The solar cell absorbs energy from sunlight and converts it into electricity. The process of converting light energy into electrical energy is called the photovoltaic effect [5]. The datasheet provided by the manufacturer lacks several important parameters needed for mathematical modeling of the device [5]. In comparison with the voltage and current characteristics of the PV and fuel cell are of nonlinear characteristics [6]. In the design of PV structures, accurate calculation of parameter values is of crucial importance [7–9]. The vast majority of studies conducted on the topic of parameter evaluation for fuel cells have focused on meta-inference, with few papers on computational methods. This is due to the fact that besides the lack of correlation in the descriptive Equations, there are a large number of unknown parameters. This makes parameter extraction an ideal problem for black box methods such as meta-inference. Several meta-heuristic approaches for estimating fuel cell parameters have been described. For example, Grasshopper optimization algorithm (GOA) [10], Salp Swarm Algorithm (SSA) [11], Multi-Verse Optimizer (MVO) [12], Grey Wolf Optimizer (GWO) [13], Modified Particle Swarm Optimizer (MPSO) [14], Hybrid Teaching Learning Based Optimization (TLBO-DE) [15], Marine Predator Algorithm (MPA) [3], Harmony Search Algorithm (HAS) [16], Barebones Particle Swarm Optimizer (BPSO) [17], have all been implemented to enhance the extraction of fuel cell parameters.

Metaheuristic optimization algorithms are completely dependent on population-based iterative approaches. They have the ability to address specific dynamic issues and do not place constraints on problem formulation. The majority of meta-heuristic methods for determining solar PV design parameters have been recently published in the literature [18].

To name few examples of popular algorithms: Genetic Algorithm based on non-uniform mutation (GAMNU) [19], Particle Swarm Optimization (PSO) algorithm [20,21], Greedy Algorithm [22,23], Cuckoo Search Ant Colony Algorithm (CSACA) [24], Bio-inspired Algorithm (BA) [25], Artificial Bee Colony (ABC) algorithm [26,27], Bacterial Foraging Optimization (BFO) algorithm [28,29], Levy Flight Based Grasshopper Optimization Algorithm (LGOA) [30], Flower Pollination Algorithm (FPA) [31,32], Jaya Optimization (JAYA) Algorithm [33,34], Either-Or Teaching Learning Based Algorithm (EOTLBO) [35], Bird Mating Optimization (BMO) Algorithm [36], teaching-leaning-based optimization (TLBO) algorithm [37,38], Nelder-Mead Simplex Algorithm Based On Eagle Strategy (NMSBES) [39], Camel Behavior Search Algorithm (CA) [40], Hybrid RAO Optimizer (HROA) [41], Political Optimizer (PO) algorithm [42], Fractional Order Darwinian Particle

Table 1
Literature survey of hybrid algorithm.

Algorithm	Application	Results
Improved Social Spider [58]	Solar cells and fuel cell	RMSE for solar is 9.86e-04 (single diode) and 9.82e-04 (double diode). Similarly, RMSE for fuel cell is 9.83e-04
Biogeography with mutation strategies [59]	Solar cells and fuel cell	RMSE for solar is 9.82e-04 (single diode) and 9.86e-04 (double diode). Similarly, SSE for fuel cell is 7.61
Improved Teaching Learning Based Optimization with elite strategy [60]	Solar cells and fuel cell	RMSE for solar is 9.86e-04 (single diode). Similarly, SSE for fuel cell is 7.62
Hybrid Particle swarm optimization RAT [67]	Solar cells and fuel cell	RMSE for solar is 8.72e-08 (modified three diode). Similarly, SSE for fuel cell is 1.04e-10

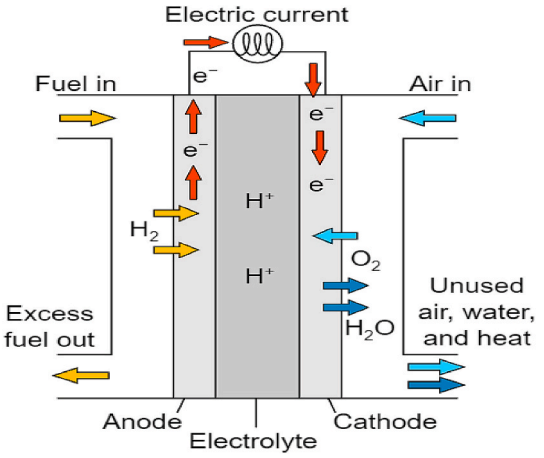

Fig. 1. Schematic diagram of the PEMFC model.

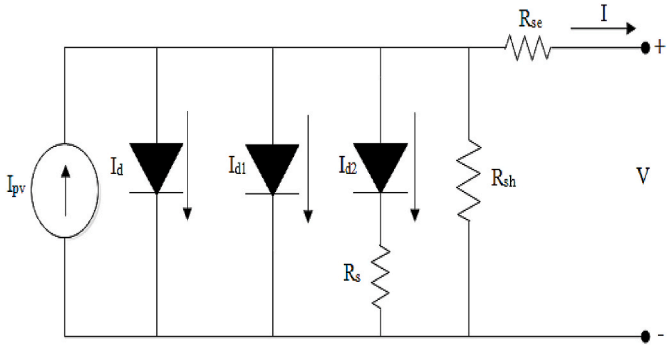

Fig. 2. Equivalent circuit of the triple-diode PV model.

Swarm Optimization (FODPSO) [43], Improved Equilibrium Optimizer (IEO) [44], Adaptive Slime Mould Algorithm (ASMA) [45], Imperialist Competitive Algorithm (ICA) [46], Harmony Search (HS) algorithm [47], Firefly Algorithm (FA) [48], Chaotic Gradient-Based Optimization (CGBO) [49], Moth-Flame Optimization (MFO) [50], Water Cycle Algorithm (WCA) [51,52], Shuffled Frog Leaping (SFL) algorithm [53], Metaphor-less Algorithm [54]. Compared with analytical and numerical methods, meta-heuristic approaches may yield adequate outcomes for estimating the characteristics of solar PV cells. Since the parameter extraction problem for a solar cell is a multi-modal optimization problem, the dependability of such descriptive approaches needs to be increased. Both meta-heuristic and deterministic techniques are among

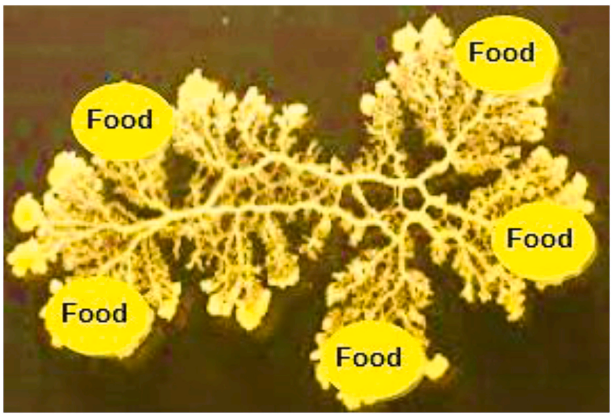

Fig. 3. Slime Mould foraging morphology.

Table 2
List of chaotic maps.

Map Name	Definition	Referred Algorithm
Chebyshev map	$x_{k+1} = \cos\left(k\cos^{-1}(x_k)\right)$	HCPSOSMA1
Logistic map	$x_{k+1} = ax_k(1-x_k)$	HCPSOSMA 2
Sine map	$x_{k+1} = \frac{a}{4}\sin(\pi x_k)$	HCPSOSMA 3
Singer map	$x_{k+1} = \mu(7.86x_k - 23.31x_k^2 + 28.75x_k^3 - 13.3028.75x_k^4$	HCPSOSMA 4
Sinusoidal map	$x_{k+1} = ax_k^2\sin(\pi x_k)$	HCPSOSMA 5

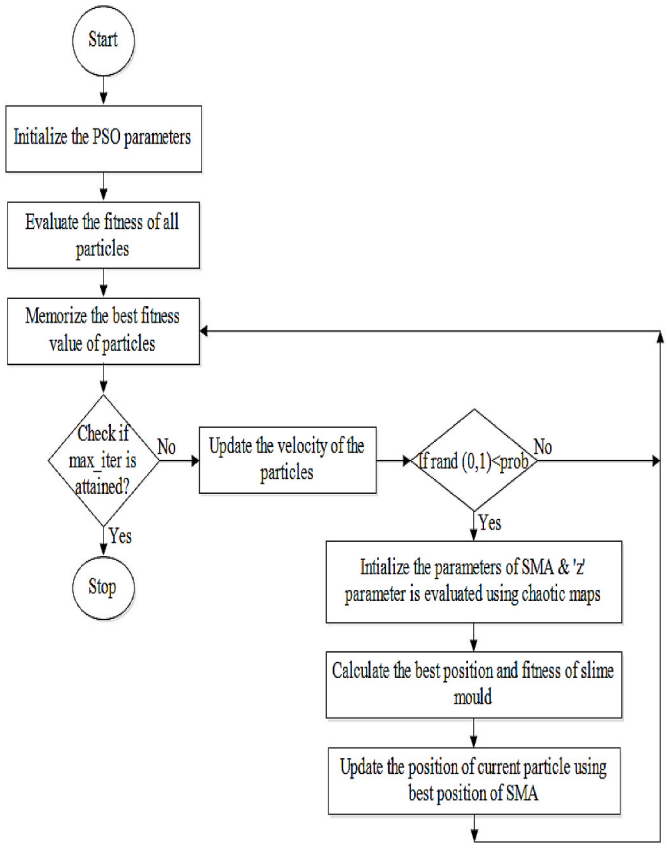

Fig. 4. Flow chart of HCPSOSMA.

Initialize all parameters

For i=1 to max_iter

Run PSO

Update the velocity of particles

If rand (0,1) < prob, then (to avoid local minima)

Initialize the parameters of SMA where 'z' parameter is evaluated using chaotic maps

Run SMA

Calculate the best position and fitness

Update the position of current particle according to best position

end

Fig. 5. Pseudo code of HCPSOSMA.

Table 3
Algorithm parameters and values.

Algorithm	Parameters	Values
HCPSOSMA	Search agents	50
	Maximum iteration	1000
	Cognitive component (c_1)	Varied using chaotic maps
	Social component (c_2)	1.5
	Minimum inertia weight	0.4
	Maximum inertia weight	0.9
	z	0.03
PSO	Search agents	50
	Maximum iteration	1000
	Cognitive component (c_1)	1.5
	Social component (c_2)	1.5
	Minimum inertia weight	0.4
	Maximum inertia weight	0.9
SMA	Search agents	50
	Maximum iteration	1000
	z	0.03
ALO	Search agents	50
	Maximum iteration	1000
	cMin	0.00004
ASO	Search agents	50
	Maximum iteration	1000
	Population of atoms (Atom_pop)	rand(Atom_Num,Dim).*(Up-Low) + Low
	Velocity of atoms (Atom_V)	rand(Atom_Num,Dim).*(Up-Low) + Low
HHO	Search agents	50
	Maximum iteration	1000
	E1	2*(1-(t/T))
	E0	2*rand-1 (range lies between −1 and 1)

the most frequently used types of PEMFC and PV cell parameter evaluation methods. Least square method [55], Lambert W-function [56], and iterative curve fitting [57] are examples of deterministic methodologies. The strength of these techniques is how quickly they can come up with estimates. On the other hand, their solutions are very sensitive to the initial solutions and sometimes lead to local optimum outcomes. The Table 1 shows the comparison of the different proposed algorithm in the literature who has done work on both the applications.

Table 4
Benchmark test function.

Name of Function	Function	Range	Dimension
f_1 = Sphere	$f_1(y) = \sum_{j=1}^{m} y_j^2$	[-100,100]	m = 30
f_2 = Schwefel 2.22	$f_2(y) = \sum_{j=1}^{m} \lvert y_j \rvert + \prod_{j=1}^{m} \lvert y_j \rvert$	[-10,10]	m = 30
f_3 = Schwefel 1.2	$f_3(y) = \sum_{j=1}^{m} \left(\sum_{i=1}^{j} y_i \right)^2$	[-100,100]	m = 30
f_4 = Schwefel 2.21	$f_4(y) = max_j \{ \lvert y_j \rvert, 1 \le j \le m \}$	[-100,100]	m = 30
f_5 = Rosenbrock	$f_5(y) = \sum_{j=1}^{m} 100 \left(y_j + 1 - y_j^2 \right)^2 + \left(y_j - 1 \right)^2$	[-30,30]	m = 30
f_6 = Step	$f_6(y) = \sum_{j=1}^{m} \left(\lfloor y_j + 0.5 \rfloor \right)^2$	[-100,100]	m = 30
f_7 = Quartic	$f_7(y) = \sum_{j=1}^{m} j y_j^4 + randm\,[0,1]$	[-128,128]	m = 30
f_8 = Schwefel	$f_8(y) = \sum_{j=1}^{m} -y_j \, Sin\left(\sqrt{\lvert y_j \rvert} \right)$	[-500,500]	m = 30
f_9 = Rastrigin	$f_9(y) = \sum_{j=1}^{m} \left[y_j^2 - 10 \, Cos\left(2\pi y_j \right) + 10 \right]$	[-5.12,5.12]	m = 30
f_{10} = Ackley	$f_{10}(y) = -20 \, exp\left(-0.2 \left(\frac{1}{m} \sum_{j=1}^{m} y_j^2 \right)^{\wedge} 0.5 \right) - exp\left(\frac{1}{m} \sum_{j=1}^{m} Cos\left(2\pi y_j \right) \right) + 20 + e$	[-32,32]	m = 30

The key purpose of this paper is to establish a new parameter extraction approach for both PEM fuel cell based-solar PV cell models. The following is a synopsis of the most important contributions made by this paper:

- A novel metaheuristic efficient hybrid algorithm (HCPSOSMA), which is chaotically varied using five maps. By eliminating the possibility of reaching a local minimum, these hybrid chaotic maps contribute to increasing the accuracy of the proposed method.
- The suggested algorithm includes a novel function known as "outstanding mathematical model of adaptive weights" that stimulates negative and positive inputs from the spread wave to determine the ideal approach to link food with an excellent exploitation propensity and exploration ability.
- The objective function for evaluating the proton exchange membrane fuel cell is the Sum of Square Error (SSE).
- Root Mean Square Error (RMSE) describes the fitness function for the estimation of triple-diode PV parameters.
- The extraction and error of the parameters are computed using the hybrid chaotic particle swarm optimization slime mould algorithm family. The convergence curves together with the I–V characteristics curves and the P–V characteristics curves demonstrate the performance and dependability of the presented approach.
- Additionally, non-parametric statistical tests are carried out to provide further insight into the results of the obtained parameters.

Table 5
Statistical results of benchmark test function.

Algorithm		F_1	F_2	F_3	F_4	F_5	F_6	F_7	F_8	F_9	F_{10}
HCPSOSMA1	Mean	0.00E+ 00	2.77E-301	0.00E+ 00	3.74E-216	2.27E-04	3.70E-30	3.23E-07	−9348.72	0.00E+ 00	8.88E-20
	S.D.	0.00E+ 00	0.00E+ 00	0.00E+ 00	0.00E+ 00	5.74E- 06	3.16E-30	2.24E-07	1.88E-12	0.00E+ 00	1.25E-35
PSO	Mean	6.44E+ 00	39.56	18720.91	29.94	10119.97	4.84E+ 00	6.95E-02	−605.519	111.23	11.74
	S.D.	4.23E+ 00	51.98	8393.92	26.23	13698.16	2.27E-01	2.71E-02	78.67	31.41	9.91
SMA	Mean	0.00E+ 00	2.16E-206	0.00E+ 00	9.71E-210	1.62E- 03	3.58E-25	1.14E-04	−12569.4	0.00E+ 00	8.88E-16
	S.D.	0.00E+ 00	0.00E+ 00	0.00E+ 00	0.00E+ 00	2.26E- 03	2.64E-25	9.35E-05	6.27E-02	0.00E+ 00	2.04E-31
ALO	Mean	1.75E- 06	14.83	519.50	10.02	71.17	2.41E- 06	2.52E-02	−5993.01	82.12	2.52
	S.D.	1.46E- 06	26.37	202.07	2.56	96.61	1.97E- 06	1.74E-02	913.56	22.02	1.31
ASO	Mean	4.69E- 03	9.53E-06	3051.03	19.28	63.40	4.51E+ 00	2.40E-03	−3861.83	19.46	1.53
	S.D.	1.41E- 02	1.33E-05	3496.81	13.59	116.76	4.67E- 01	1.28E-03	141.95	26.35	4.41E-01
HHO	Mean	3.59E-37	1.11E-12	3.14E-23	0.76	2853.616	1.82E-02	4.35E-03	−7547.42	101.55	2.43E-04
	S.D.	1.33E-36	3.35E-13	5.22E-23	0.27	2476.887	3.96E-02	2.23E-03	596.68	19.96	6.77E-04

Table 6
Upper and lower bounds of the PEMFC Model parameters.

Parameter	Lower bound	Upper bound
ξ_1	−1.1997	−0.08532
ξ_2*10-3	0.8	6.00
ξ_3*10-5	3.60	9.80
ξ_4*10-4	−2.60	−0.954
λ	10.00	24.00
RC*10-4	1.00	8.00
b	0.0136	0.5

Table 7
Datasheet of the PEMFC manufacturer.

Model	Ballard Mark V
n	35
A [cm2]	50.6
l [μm]	178
Jmax [A/cm2]	1.5
PH2 [bar]	1
PO2 [bar]	1
Power [W]	1000
T [°K]	343.15
Anode volume [m3]	0.005
Cathode volume [m3]	0.01
Membrane dry density [kg/cm3]	0.002
Membrane dry Eq. weight [kg/mol]	1.1

Table 9
Statistical results of the PEMFC model.

Algorithms	Minimum	Average	Maximum	Mean	Standard Deviation
HCPSOSMA1	1.00E-15	4.01E-15	8.84E-15	4.01E-15	2.44E-15
HCPSOSMA 2	1.05E-16	3.78E-16	8.06E-16	3.78E-16	2.38E-16
HCPSOSMA 3	1.04E-15	2.97E-15	9.19E-15	2.97E-15	2.12E-15
HCPSOSMA 4	1.09E-15	3.26E-15	9.66E-15	3.26E-15	2.42E-15
HCPSOSMA 5	1.08E-16	4.16E-16	8.12E-16	4.16E-16	2.26E-16
PSO	5.21E-03	6.46E-03	7.15E-03	6.46E-03	0.00053
SMA	1.15E-05	1.80E-05	2.70E-05	1.80E-05	4.67E-06
ALO	1.02E-04	1.63E-04	2.95E-04	1.63E-04	6.58E-05
ASO	1.01E-04	1.52E-04	2.19E-04	1.52E-04	3.46E-05
HHO	1.01E-04	1.75E-04	2.84E-04	1.75E-04	5.16E-05

2. Mathematical model of PEMFC stack

PEMFCs are typically built with cathode and anode electrodes separated by a polymer electrolyte membrane that limits electron flow. Fig. 1 depicts the process of injecting hydrogen from the anode side and

Table 8
PEMFC parameter evaluation results.

Parameter/ Algorithms	ξ_1	ξ_2	ξ_3	ξ_4	λ	RC	b	Wilcoxon's rank sum test	SSE	Computational time (sec)
HCPSOSMA1	−1.03937	0.00356	6.31E-05	−0.00017	15.2262	0.00033	0.16979		4.01E-15	2.78
HCPSOSMA 2	−1.02938	0.00328	6.10E-05	−0.00020	17.5889	0.00053	0.32718		3.78E-16	2.95
HCPSOSMA 3	−1.02245	0.00304	6.42E-05	−0.00020	16.8555	0.00053	0.28344		2.97E-15	2.81
HCPSOSMA 4	−0.99965	0.00303	5.81E-05	−0.00020	16.3778	0.00045	0.31125		3.26E-15	2.99
HCPSOSMA 5	−1.02253	0.00280	5.73E-05	−0.00019	18.2587	0.00049	0.27149		4.16E-16	2.85
PSO	−0.97358	0.00260	7.11E-05	−0.00020	16.2515	0.00033	0.21801	+	6.46E-03	1.54
SMA	−1.19439	0.00105	4.11E-05	−0.00017	15.0415	0.00025	0.20280	+	1.80E-05	1.23
ALO	−1.03760	0.00321	6.87E-05	−0.00017	17.70551	0.00047	0.31015	+	1.63E-04	1.62
ASO	−1.04598	0.00311	6.63E-05	−0.00018	17.25200	0.00039	0.29674	+	1.52E-04	1.30
HHO	−1.04155	0.00219	6.06E-05	−0.00016	14.07131	0.00032	0.17212	+	1.75E-04	1.66

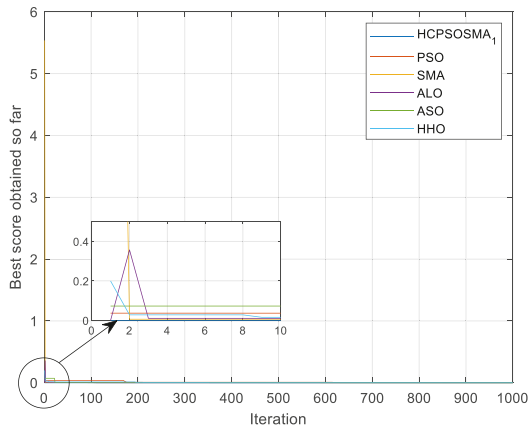

Fig. 6. Convergence curves of the PEMFC algorithms.

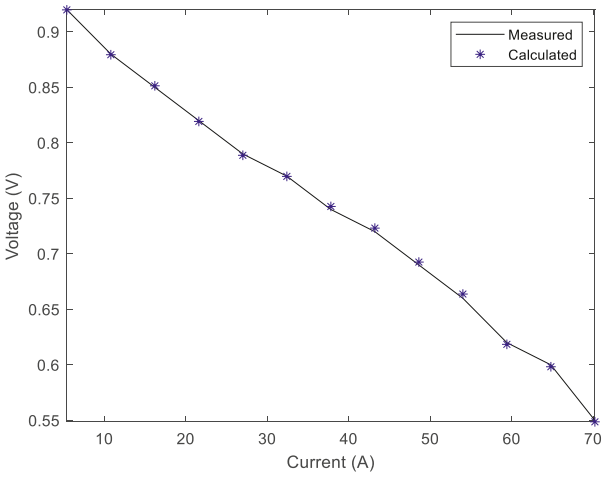

HCPSOSMA1

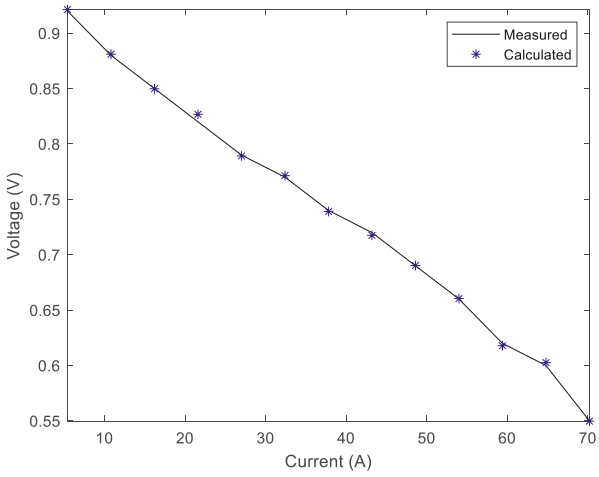

HCPSOSMA2

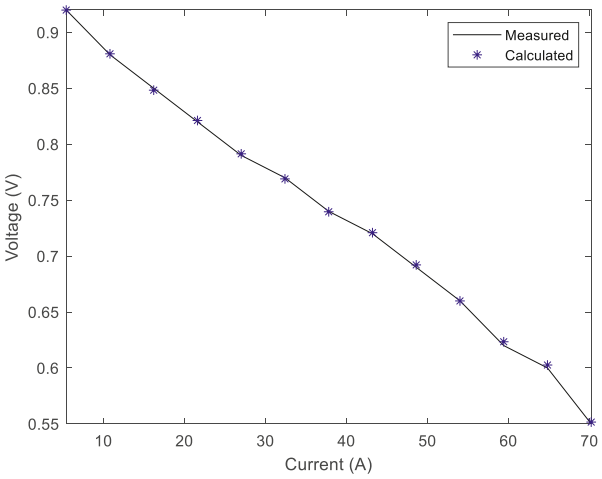

HCPSOSMA3

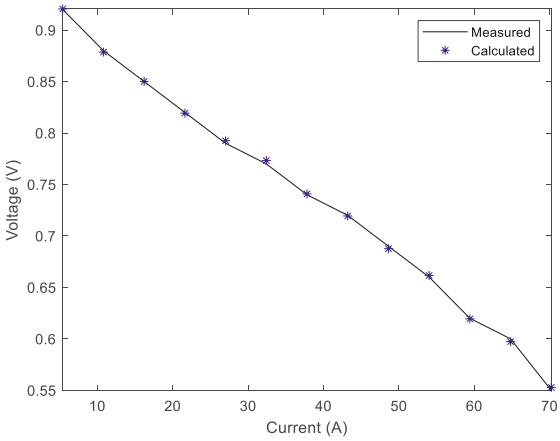

HCPSOSMA4

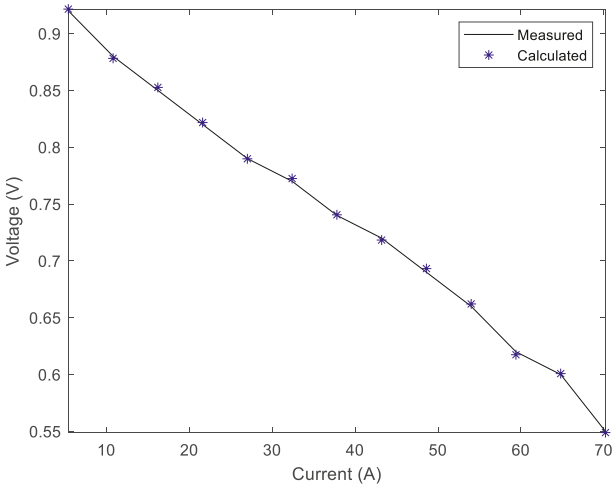

HCPSOSMA5

Fig. 7. The V–I curves of the PEMFC model.

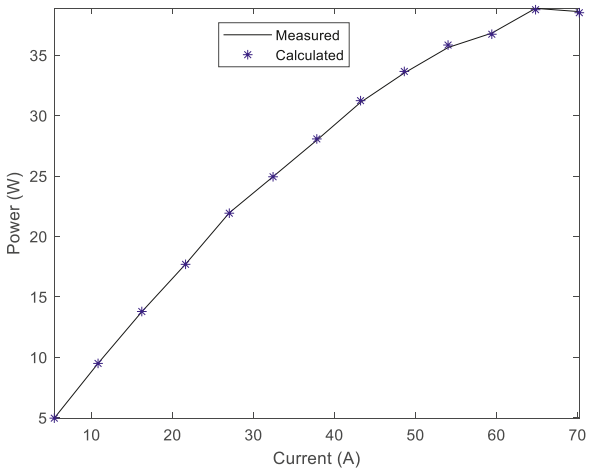

HCPSOSMA1

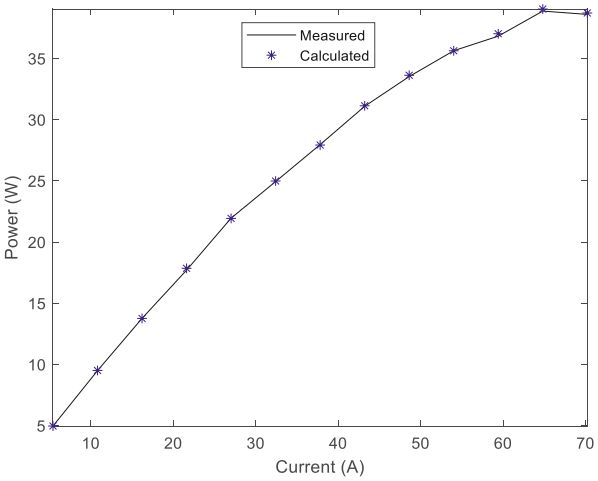

HCPSOSMA2

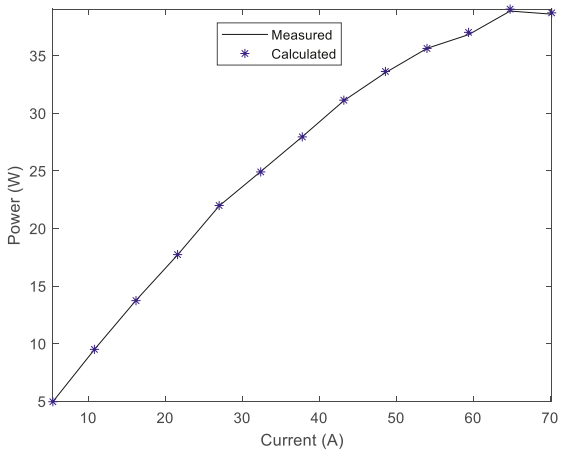

HCPSOSMA3

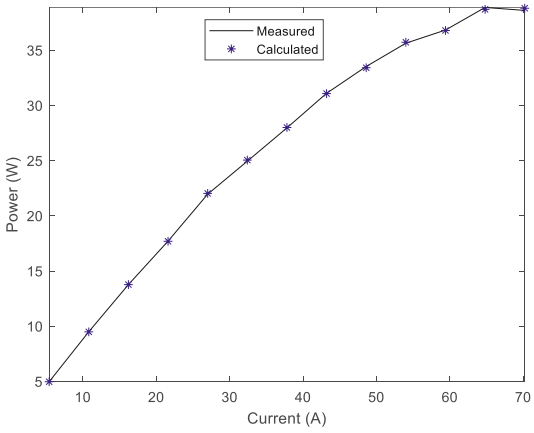

HCPSOSMA4

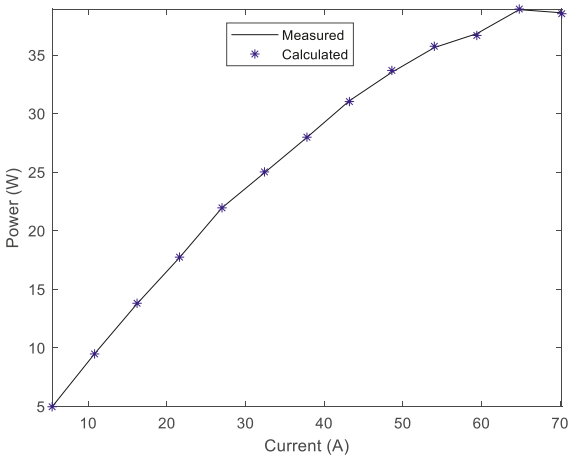

HCPSOSMA5

Fig. 8. The P–I curves of the PEMFC model.

Table 10
Statistical results based on Friedman ranking test.

Algorithms	Friedman Ranking	Final Ranking
HCPSOSMA1	112.933	5
HCPSOSMA 2	28	1
HCPSOSMA 3	99	3
HCPSOSMA 4	103.5	4
HCPSOSMA 5	32.333	2
PSO	285.166	10
SMA	165	6
ALO	221.266	7
ASO	222.266	8
HHO	231.866	9

supplying oxygen from the cathode side [61]. The electrochemical processes that occur at the electrodes of PEMFCs are described by the Equations [61,62]:

Anode side:

$$H_2 \rightarrow 2H^+ + 2e^- \tag{1}$$

Cathode side:

$$2H^+ + \frac{1}{2}O_2 \rightarrow H_2O \tag{2}$$

Overall chemical reaction:

$$2H^+ + \frac{1}{2}O_2 \rightarrow H_2O + \text{energy} \tag{3}$$

The output current and voltage of a single PEMFC stack are quite small. As a result, numerous stacks must be merged and connected, either in series or parallel, according to specifications, in order to create a significant amount of energy. Equation (4) defines the stack output voltage when connected in series.

$$V_{stack} = N_{cells} * V_{cell} \tag{4}$$

where N_{cells} denotes the number of cells connected in series and V_{cell} denotes the voltage of each cell.

The terminal output voltage of each fuel cell is primarily composed of three types of voltage: activation voltage drop ($V_{activation}$), ohmic voltage drop (V_{ohmic}), and concentration voltage drop ($V_{concentration}$). Equation (5) mentions the output voltage of a single fuel cell.

$$V_{cell} = E_{Nernst} - V_{activation} - V_{ohmic} - V_{concentration} \tag{5}$$

where E_{Nernst} represents the open circuit voltage and Equation (6) reflects the mathematical form of E_{Nernst} as follows:

$$E_{Nernst} = 1.229 - 0.85 \times 10^{-3}(T_{fc} - 298.15) + 4.3085 \times 10^{-3} T_{fc} \times \left[\ln(P_{H2}) + \ln\left(\sqrt{P_{O2}}\right)\right] \tag{6}$$

where T_{fc} is the operating cell temperature and P_{O2} and P_{H2} are the partial pressures of oxygen and hydrogen at the inlet channels in the fuel cell stack. The pressures can be calculated as follows:

$$P_{H2} = 0.5(PH_a \times P_{H2O})\left[\left(\exp\left(\frac{1.635\left(\frac{I_{fc}}{A}\right)}{T_{fc}^{1.334}}\right) \times \frac{(PH_a \times P_{H2O})}{P_a}\right)^{-1} - 1\right] \tag{7}$$

$$P_{O2} = (RH_C \times P_{H2O})\left[\left(\exp\left(\frac{4.192\left(\frac{I_{fc}}{A}\right)}{T_{fc}^{1.334}}\right) \times \frac{(PH_a \times P_{H2O})}{P_c}\right)^{-1} - 1\right] \tag{8}$$

where P_a and P_c represent the pressure at the anode and cathode of the input channel, respectively; PH_a and RH_C represent the relative vapour humidity around the anode and cathode, respectively; I_{fc} represents the current generated by the cell, A represents the surface area of the membrane, and P_{H2O} represents the water saturation pressure, which can be represented by Equation (9):

$$P_{H2O} = 2.95 \times 10^{-2}(T_{fc} - 273.15) - 9.18 \times 10^{-5}(T_{fc} - 273.15)^2 + 1.44 \times 10^{-7}(T_{fc} - 273.15)^3 - 2.18 \tag{9}$$

The voltage loss $V_{activation}$ caused by the activation process can be computed using Equation (10):

$$V_{activation} = -\left[\xi_1 + \xi_2 T_{fc} + \xi_3 T_{fc} \ln(C_{O2}) + \xi_3 T_{fc}\, ln\ln(I_{fc})\right] \tag{10}$$

where the semi-empirical coefficients are given by ξ_1, ξ_2, ξ_3, ξ_4; on the cathode side, the oxygen concentration is denoted by C_{O2} and is computed as illustrated in Equation (11):

$$C_{O2} = \frac{P_{O2}}{5.08 \times 10^6 \times exp^{-\left(\frac{498}{T_{fc}}\right)}} \tag{11}$$

The resistive ohmic voltage drop is represented by Equation (12), in which the membrane surface resistance is denoted by R_M and the resistance connection is denoted by R_C and the membrane resistance is given in Equation (13).

$$V_{ohmic} = I_{fc}(R_M + R_C) \tag{12}$$

$$R_M = \frac{\rho M \times l}{A} \tag{13}$$

where ρM is the specific resistance of the membrane material, l denotes the membrane thickness, and ρM is given in Equation (14) as:

$$\rho M = \frac{181.6\left[1 + 0.03\left(\frac{I_{fc}}{A}\right) + 0.062\left(\frac{T_{fc}}{303}\right)^2\left(\frac{I_{fc}}{A}\right)^{2.5}\right]}{\left[\lambda - 0.634 - 3\left(\frac{I_{fc}}{A}\right)\right] \times exp\left[4.18\left(\frac{T_{fc}-303}{T_{fc}}\right)\right]} \tag{14}$$

where λ is the adjustable empirical variable. $V_{concentration}$ is expressed in Equation (15) as:

$$V_{concentration} = -b\, ln\left(1 - \frac{J}{Jmax}\right) \tag{15}$$

where b represents the parametric variable and $Jmax$ represents the maximum current density.

Certain parameters, in general, are not defined in the vendor's datasheet. Accurate study of these factors is thus critical for ensuring adequate modeling of PEMFC under control and operation. The PEMFC model, in particular, comprises seven unknown parameters $\xi_1, \xi_2, \xi_3, \xi_4$, λ, RC, and b. The unknown parameters are designed to have the best values between their lower and upper boundaries using the proposed algorithm.

2.1. Problem formulation of PEMFC model

In order to create the PEMFC model, a new method is utilized to match the anticipated output with the actual result. In this research, the Sum of Squared Error (SSE) was employed as a measure to compare the mathematical model output voltage to the practical output voltage. Equation (16) is a representation of the objective function that this article aims to accomplish.

$$\text{Min}\left(\mathrm{F} = \sum_{\mathrm{i}=1}^{\mathrm{N}} (\mathrm{V}_{\text{actual}} - \mathrm{V}_{\mathrm{i}})^2\right) \tag{16}$$

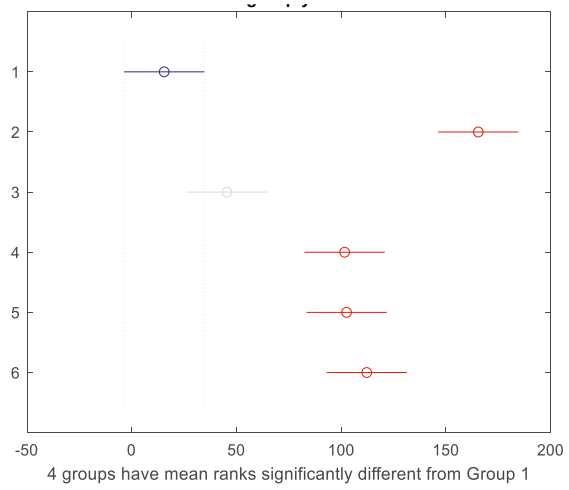

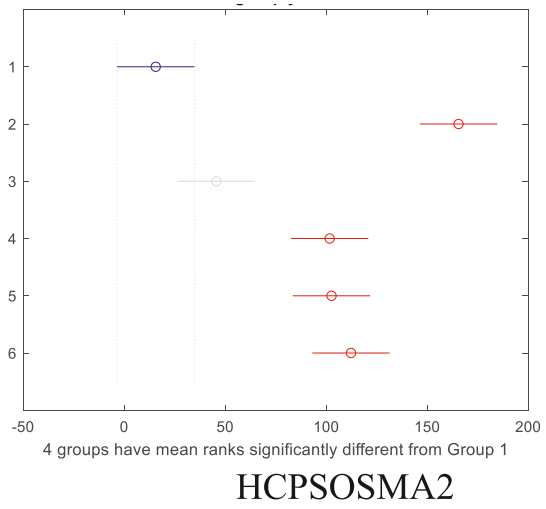

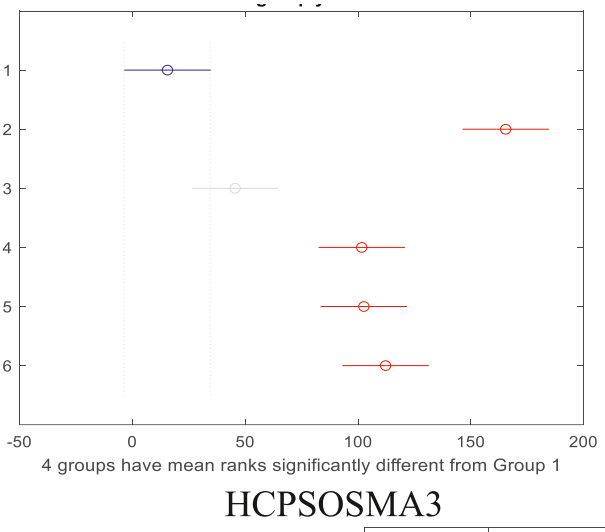

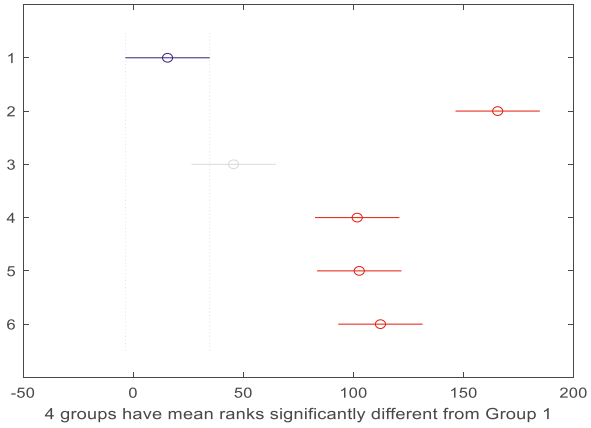

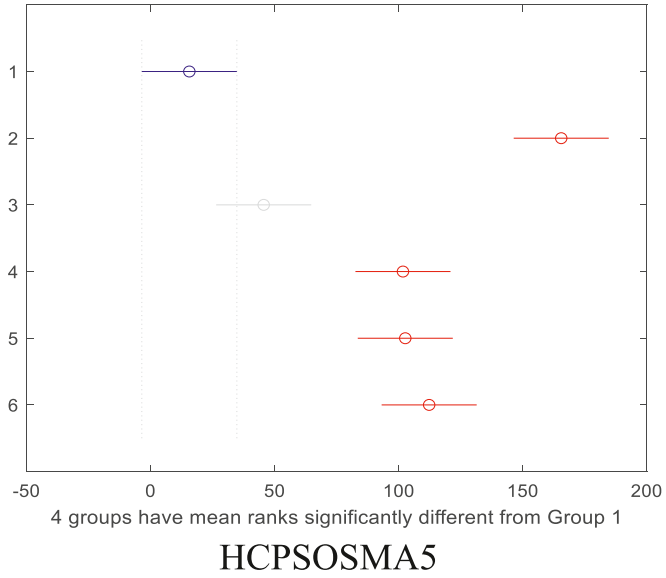

Fig. 9. The Ballard Mark-V Mean Ranking determined using the Kruskal-Wallis Test.

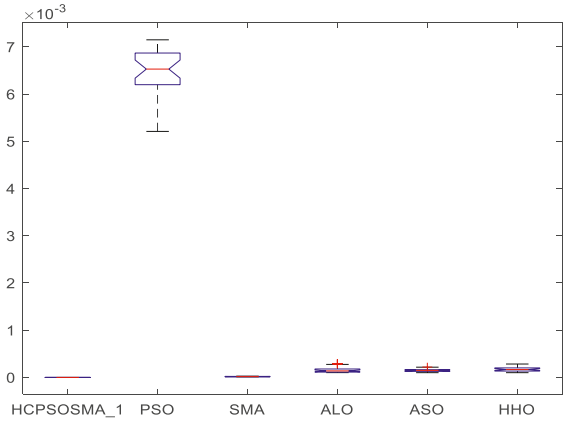

HCPSOSMA1

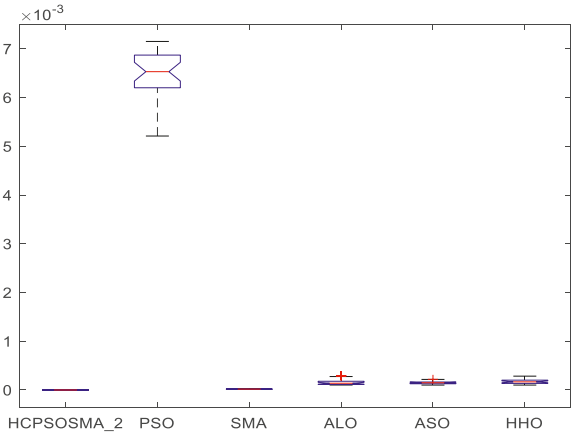

HCPSOSMA2

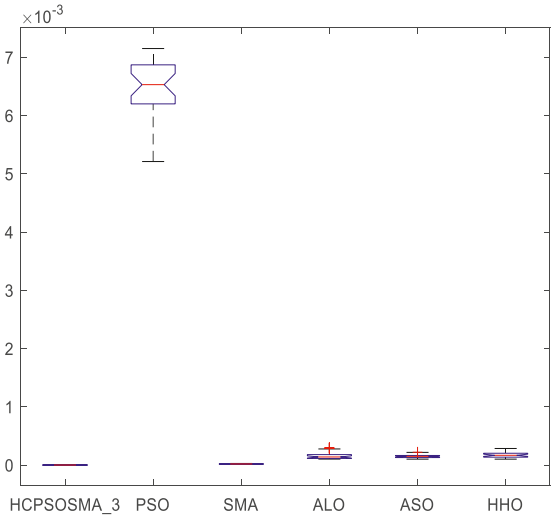

HCPSOSMA3

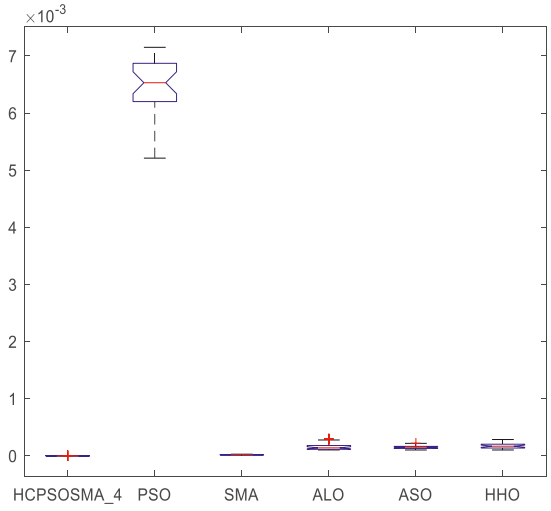

HCPSOSMA4

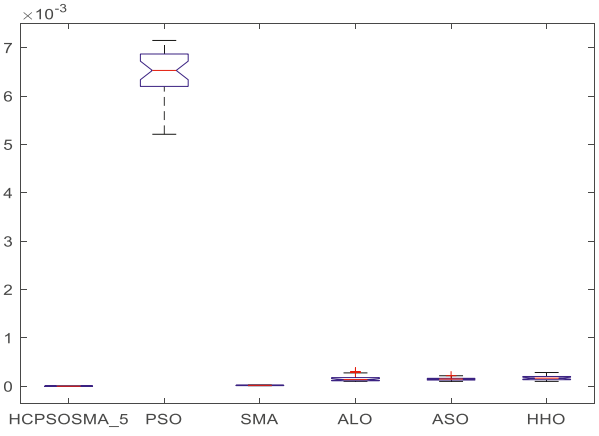

HCPSOSMA5

Fig. 10. The Ballard Mark-V Median Ranking determined using the Kruskal-Wallis Test.

Table 11
Mood's median test for Ballard Mark-V.

SOURCE	SS	DF	MS	Chi-sq	Prob > Chi-sq	Algorithm
Columns	420553.3	5	84110.7	154.92	1.19E-31	HCPSOSMA1
Error	65360.7	174	375.6	–	–	
Total	485,914	179	–	–	–	
Columns	420553.3	5	84110.7	154.92	1.195E-31	HCPSOSMA2
Error	65360.7	174	375.6	–	–	
Total	485,914	179	–	–	–	
Columns	420553.3	5	84110.7	154.92	1.193E-31	HCPSOSMA3
Error	65355.2	174		375.6-	–	
Total	485908.5	179	–	–	–	
Columns	420553.3	5	84110.7	154.92	1.195E-31	HCPSOSMA4
Error	65360.7	174	375.6	–	–	
Total	485,914	179	–	–	–	
Columns	420553.3	5	84110.7	154.92	1.195E-31	HCPSOSMA5
Error	65360.7	174	375.6	–	–	
Total	485,914	179	–	–	–	

Table 12
The search range of the PV model parameters.

Parameter	Lower bound	Upper bound
Ipv (A)	0	1
Io1, Io2, Io3 (uA)	0	1
Rs (ohm)	0	0.5
Rsh (ohm)	0	100
Alpha1, Alpha2, Alpha3	1	2

Table 13
The parameter estimation PV datasheet.

Company	R.T.C France
Vm [V]	0.4507
Im [A]	0.6894
Voc [V]	0.5728
Isc [A]	0.7603
Ns [Cells]	1
T [oC]	33

where V_{actual} indicates the actual experiment voltage, V_i represents the calculated model voltage and N represents the quantity of data points.

2.2. Basic PV cell MODELLIMG of triple-diode PV model

In the Triple-Diode Model (TDM), three diodes are connected in parallel in the PV cell model as represented in Fig. 2. The third diode in TDM of PV cell model is to take into account the effect of leakage current and grain boundaries.

The current (I Amp) Equation of the TDM is thus formulated in Equation (17):

$$I = I_{ph} - I_o\left[exp\left(\frac{q(V+IR_S)}{\alpha KT}\right) - 1\right] - I_{o1}\left[exp\left(\frac{q(V+IR_S)}{\alpha_1 KT}\right) - 1\right] - I_{o2}\left[exp\left(\frac{q(V+IR_S)}{\alpha_2 KT}\right) - 1\right] - \frac{V+IR_S}{R_{sh}} \quad (17)$$

The nine unidentified parameters of TDM to be extracted are $I_{ph}, I_o, \alpha, I_{o1}, \alpha_1, I_{o2}, \alpha_2, R_S, R_{Sh}$. Again, compared to DDM, there are an extra pair of factors a new method is utilized to match the anticipated output with the actual result to consider. In this work, we take into account TDM of PV cell to improve the precision of the estimation method. Following are descriptions of the open circuit, short circuit, and maximum power circumstances.

At open circuit $I = 0$ and $V = V_{OC}$; then Equation (18) becomes as follows:

Table 15
Statistical results of R.T.C France model at STC.

Algorithms	Minimum	Average	Maximum	Mean	Standard Deviation
HCPSOSMA1	1.12E-12	3.57E-12	9.47E-12	3.57E-12	2.26E-12
HCPSOSMA 2	1.16E-12	3.42E-12	7.87E-12	3.42E-12	2.31E-12
HCPSOSMA 3	1.23E-13	4.31E-13	9.42E-13	4.31E-13	2.30E-13
HCPSOSMA 4	1.01E-12	4.14E-12	9.44E-12	4.14E-12	2.16E-12
HCPSOSMA 5	1.04E-12	4.03E-12	9.54E-12	4.03E-12	2.71E-12
PSO	0.1547	0.1607	0.1644	0.1607	0.0031
SMA	1.02E-04	3.26E-04	8.93E-04	3.26E-04	2.36E-04
ALO	0.01475	0.01478	0.01479	0.01478	1.15E-05
ASO	0.00152	0.00155	0.00159	0.00155	2.18E-05
HHO	0.0014	0.00150	0.0016	0.00150	4.99E-05

Table 14
Parameter Estimation of triple-diode model at STC for RTC FRANCE.

Parameter/ Algorithm	Ipv	Alpha1	Alpha2	Alpha3	Rs	Rsh	Io1	Io2	Io3	Wilcoxon's rank sum test	RMSE	Computational time (sec)
HCPSOSMA1	0.5150	1.8196	1.8035	1.7207	0.2405	72.9892	0.0383	0.0827	0.0527		3.57E-12	2.63
HCPSOSMA 2	0.6358	1.6901	1.6123	1.9243	0.2131	81.6246	0.0027	0.1245	0.1336		3.42E-12	2.59
HCPSOSMA 3	0.4363	1.6997	1.5015	1.4757	0.3507	79.0630	0.3000	0.1168	0.0571		4.31E-13	2.68
HCPSOSMA 4	0.4058	1.6387	1.7014	1.6583	0.1012	71.8714	0.1685	0.1812	0.1321		4.14E-12	2.72
HCPSOSMA 5	0.6549	1.6000	1.7862	1.5972	0.1552	70.2889	0.0581	0.1151	0.2741		4.03E-12	2.70
PSO	0.8364	1.4192	1.5002	1.4695	0.0641	53.2430	0.4900	0.3274	0.2993	+	0.1607	1.42
SMA	0.9008	1.7460	1.5181	1.4135	0.1838	21.1449	0.5814	0.3730	0.4206	+	3.62E-04	1.18
ALO	0.8408	1.1551	1.1817	1.0358	0.1404	56.3466	0.2367	0.2882	0.2075	+	1.15E-05	1.55
ASO	0.8352	1.5226	1.3317	1.5950	0.2046	51.6181	0.3538	0.4053	0.3641	+	0.0015	1.39
HHO	0.8414	1.1735	1.1850	1.1858	0.1203	53.7050	0.2627	0.3026	0.1365		0.0015	1.68

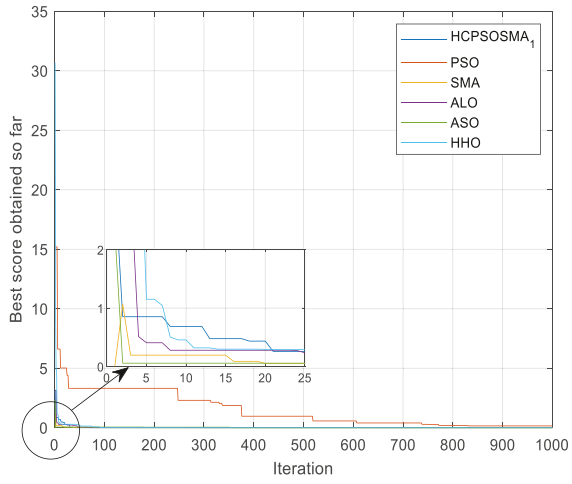

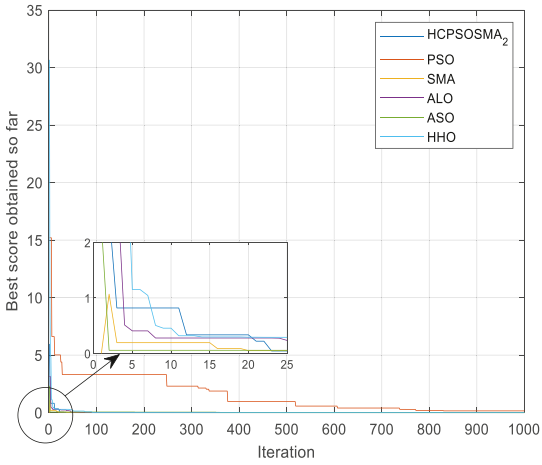

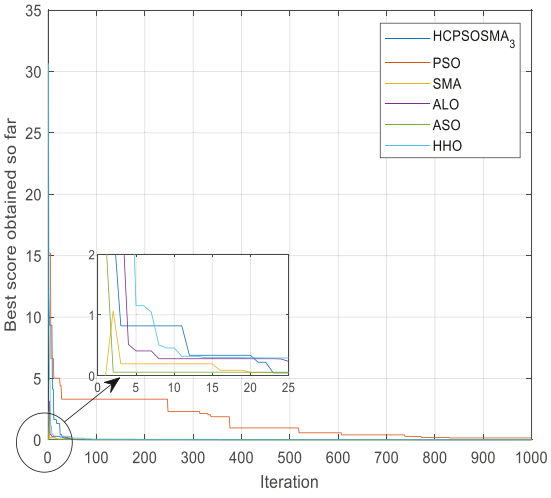

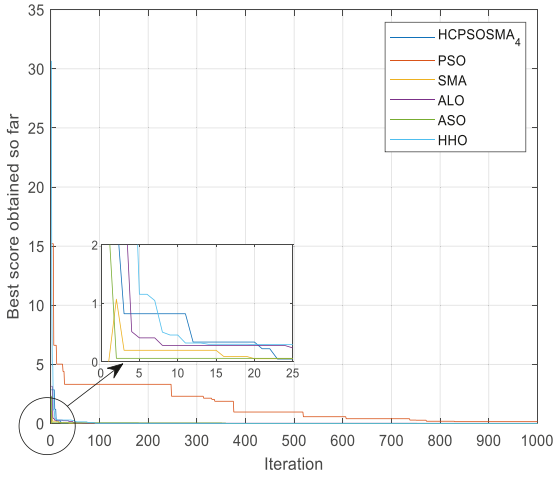

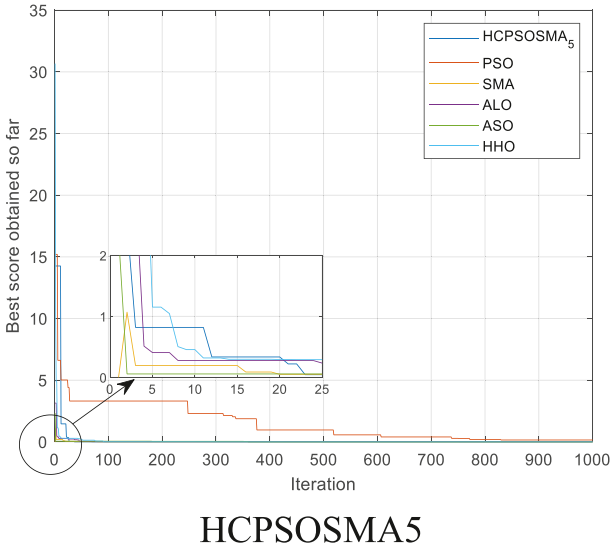

Fig. 11. Convergence curves of the solar PV model.

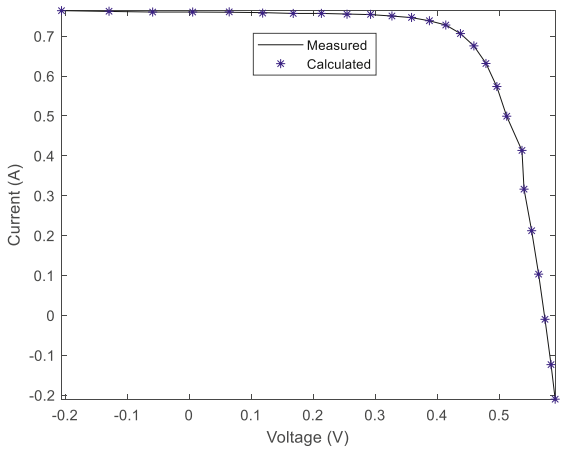

HCPSOSMA1

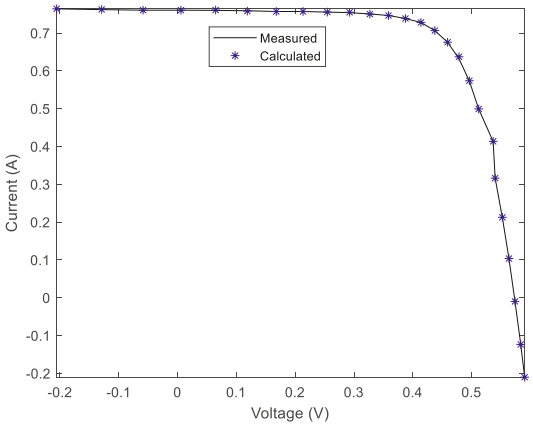

HCPSOSMA2

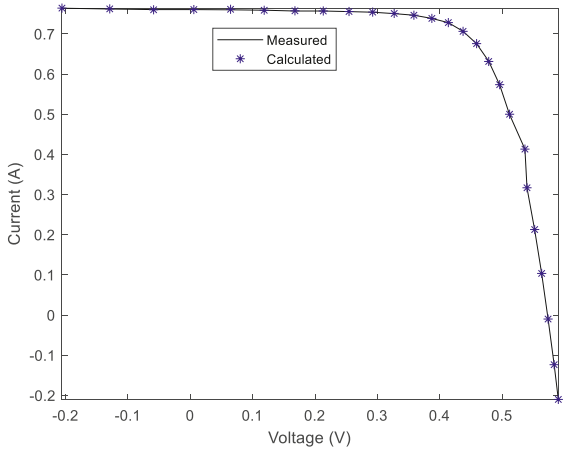

HCPSOSMA3

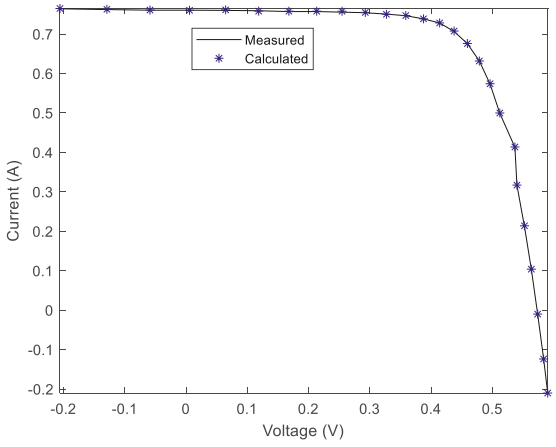

HCPSOSMA4

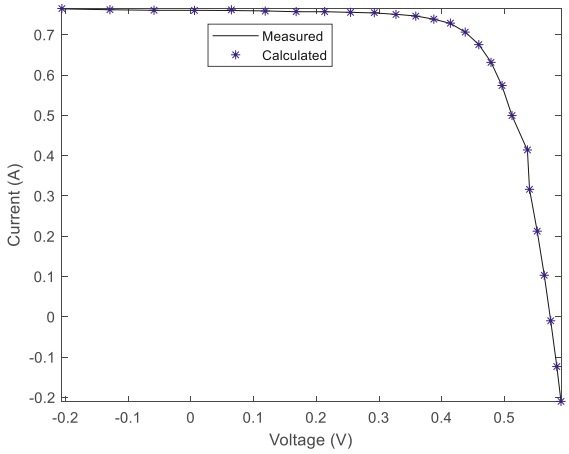

HCPSOSMA5

Fig. 12. The I–V curves of the Solar PV model.

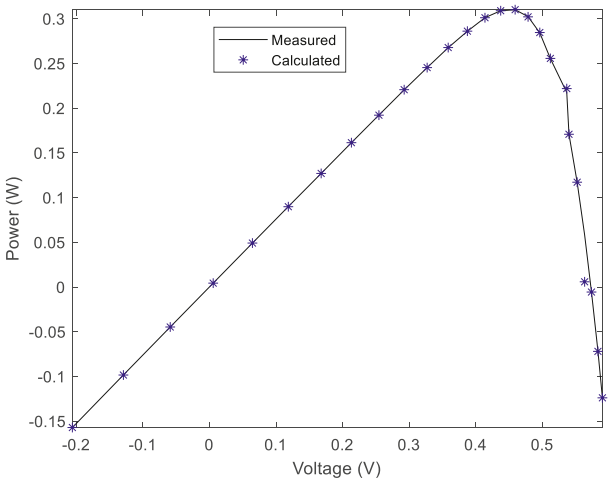

HCPSOSMA1

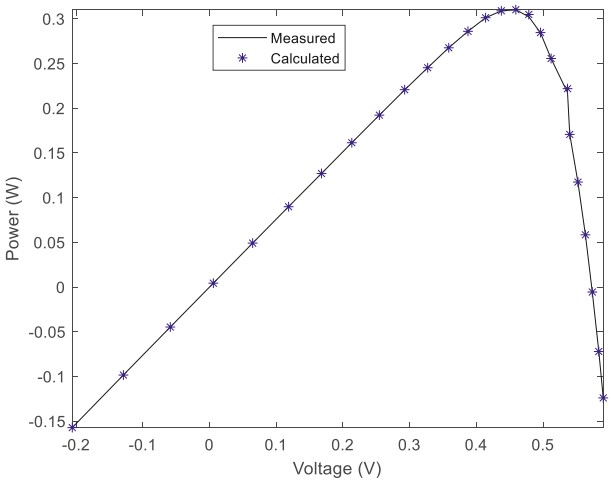

HCPSOSMA2

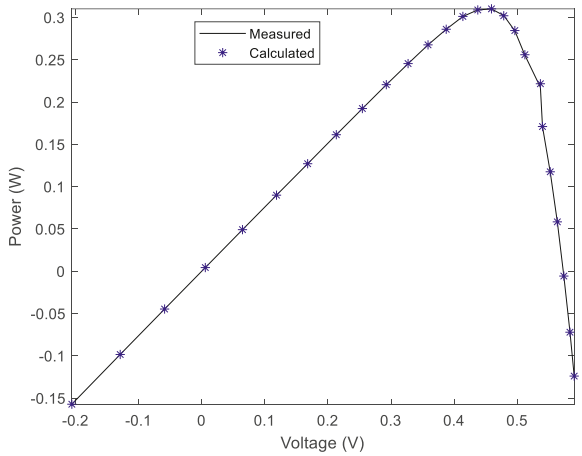

HCPSOSMA3

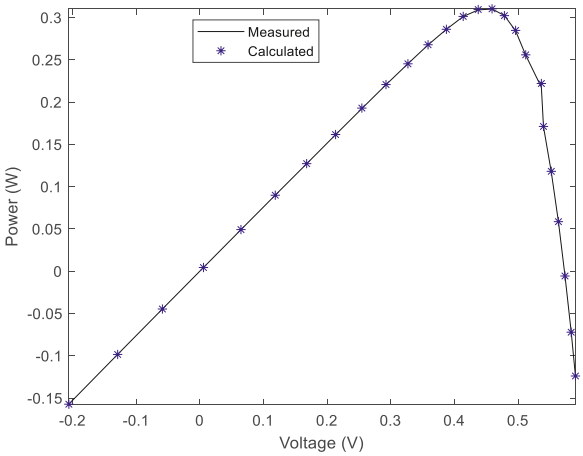

HCPSOSMA4

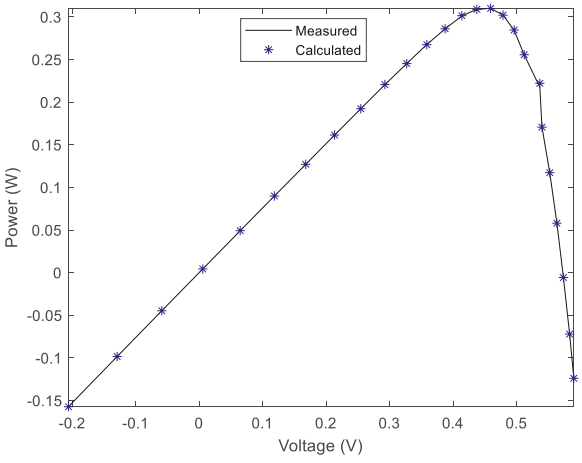

HCPSOSMA5

Fig. 13. The P–V curves of the Solar PV model.

Table 16
The statistical results for R.T.C. France solar PV cell at STC based on Friedman ranking test.

Algorithms	Friedman Ranking	Final Ranking
HCPSOSMA1	87.800	3
HCPSOSMA 2	83.466	2
HCPSOSMA 3	15.166	1
HCPSOSMA 4	98.500	5
HCPSOSMA 5	90.900	4
PSO	285.166	10
SMA	165.166	6
ALO	255.166	9
ASO	219.033	8
HHO	201.300	7

$$0 = I_{ph} - I_o\left[exp\left(\frac{qV_{OC}}{\alpha KT}\right) - 1\right] - I_{o1}\left[exp\left(\frac{qV_{OC}}{\alpha_1 KT}\right) - 1\right] - I_{o2}\left[exp\left(\frac{qV_{OC}}{\alpha_2 KT}\right) - 1\right] - \frac{V_{OC}}{R_{Sh}} \tag{18}$$

Therefore, Equation (18) becomes:

$$I_{ph} = I_o\left[exp\left(\frac{qV_{OC}}{\alpha KT}\right) - 1\right] + I_{o1}\left[exp\left(\frac{qV_{OC}}{\alpha_1 KT}\right) - 1\right] + I_{o2}\left[exp\left(\frac{qV_{OC}}{\alpha_2 KT}\right) - 1\right] + \frac{V_{OC}}{R_{Sh}} \tag{19}$$

At the time of a short circuit $V = 0$ and $I = I_{SC}$; then Equation (17) becomes as follows:

$$I_{SC} = I_{ph} - I_o\left[exp\left(\frac{qI_{SC}R_S}{\alpha KT}\right) - 1\right] - I_{o1}\left[exp\left(\frac{qI_{SC}R_S}{\alpha_1 KT}\right) - 1\right] - I_{o2}\left[exp\left(\frac{qI_{SC}R_S}{\alpha_2 KT}\right) - 1\right] - \frac{I_{SC}R_S}{R_{Sh}} \tag{20}$$

Therefore, Equation (20) will be as follows:

$$I_{ph} = I_{SC} + I_o\left[exp\left(\frac{qI_{SC}R_S}{\alpha KT}\right) - 1\right] + I_{o1}\left[exp\left(\frac{qI_{SC}R_S}{\alpha_1 KT}\right) - 1\right] + I_{o2}\left[exp\left(\frac{qI_{SC}R_S}{\alpha_2 KT}\right) - 1\right] + \frac{I_{SC}R_S}{R_{Sh}} \tag{21}$$

At maximum power point $V = V_{mp}$ and $I = I_{mp}$; then Equation (17) gives Equation (21) as follows:

$$I_{mp} = I_{sh} - I_o\left[exp\left(\frac{q(V_{mp} + I_{mp}R_S)}{\alpha KT}\right) - 1\right] - I_{o1}\left[exp\left(\frac{q(V_{mp} + I_{mp}R_S)}{\alpha KT}\right) - 1\right] - I_{o1}\left[exp\left(\frac{q(V_{mp} + I_{mp}R_S)}{\alpha KT}\right) - 1\right] - \frac{V_{mp} + I_{mp}R_S}{R_{Sh}} \tag{22}$$

2.3. Problem formulation

In this inquiry, the problem that is being looked at is trying to extract the parameters of the solar cell. In the process of formulating the objective function that will be used to evaluate the solar cell's characteristics, a number of error functions have been taken into consideration. The root mean square error (RMSE) is by far the most used measure in the literature, to verify the proposed algorithm the RMSE is considered. Within the context of this objective function, certain parameters are also determined using an analytical approach.

The RMSE is what makes up the objective function, and the following Equation describes the RMSE:

$$RMSE = \sqrt{\frac{1}{P}\sum_{I=1}^{P} f(V_{pv}, I_{pv}, Q)^2} \tag{23}$$

where Q represents the solution vector, V, and I represent the voltage and current measured, respectively. The prime objective of the presented technique is to acquire the parameters of the triple-diode model by decreasing the root mean square error. Three main conditions, mentioned earlier (open circuit, short circuit and, maximum power point), is evaluated to minimize the error using algorithms.

The open circuit error equation is presented as:

$$err_{OC} = I_o\left[\exp\left(\frac{qV_{OC}}{\alpha KT}\right) - 1\right] + I_{o1}\left[\exp\left(\frac{qV_{OC}}{\alpha_1 KT}\right) - 1\right] + I_{o2}\left[\exp\left(\frac{qV_{OC}}{\alpha_2 KT}\right) - 1\right] + \frac{V_{OC}}{R_{Sh}} - I_{ph} \tag{24}$$

The short circuit error equation is presented as:

$$err_{SC} = I_{SC} + I_o\left[exp\left(\frac{qI_{SC}R_S}{\alpha KT}\right) - 1\right] + I_{o1}\left[exp\left(\frac{qI_{SC}R_S}{\alpha_1 KT}\right) - 1\right] + I_{o2}\left[exp\left(\frac{qI_{SC}R_S}{\alpha_2 KT}\right) - 1\right] + \frac{I_{SC}R_S}{R_{Sh}} - I_{ph} \tag{25}$$

The maximum power point error equation is presented as:

$$err_{MP} = I_{sh} - I_o\left[exp\left(\frac{q(V_{mp} + I_{mp}R_S)}{\alpha KT}\right) - 1\right] - I_{o1}\left[exp\left(\frac{q(V_{mp} + I_{mp}R_S)}{\alpha KT}\right) - 1\right] - I_{o1}\left[exp\left(\frac{q(V_{mp} + I_{mp}R_S)}{\alpha KT}\right) - 1\right] - \frac{V_{mp} + I_{mp}R_S}{R_{Sh}} - I_{mp} \tag{26}$$

The RMSE can also be simply explained Equation in reference to previous Equation (23):

$$RMSE = \sqrt{mean(err_{OC}{}^2 + err_{SC}{}^2 + err_{MP}{}^2)} \tag{27}$$

Hence, the proposed heuristic approach is based on the lessening of this objective function concerning the parameter bounds.

3. Slime mould algorithm (SMA)

The slime mould is typically referred to as physarum polycephalum in this article. Since it was first identified as a fungus, it was dubbed a "slime mould," and its life cycle was first reported in a study published in 1931 by Howard [63]. The slime mould is a eukaryote that lives in cold and moist environments. The active and complicated mechanism of slime mould, plasmodium, is the major nutritional step in this article. As can be seen in Fig. 3, the slime mould reaches this stage when it begins to discover food, when it begins to surround it, and when it begins to emit enzymes that aid in digestion. The front end extends to a fan produced during migration, and it is followed by a linked vein network that permits cytoplasm to flow within [64]. The mathematical modeling of the SMA is explained in detail in Ref. [65].

3.1. Chaos theory

Chaos is a random process that occurs in a nonlinear system in

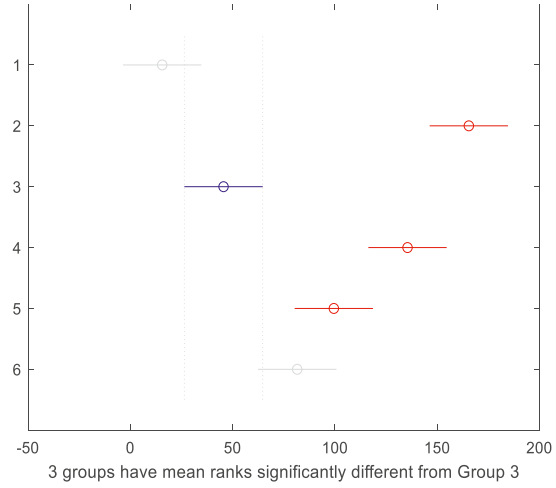

HCPSOSMA1

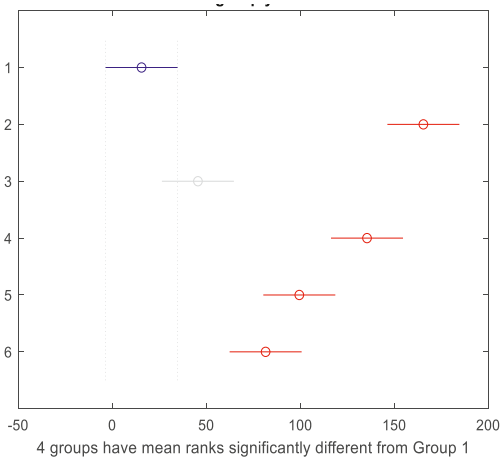

HCPSOSMA2

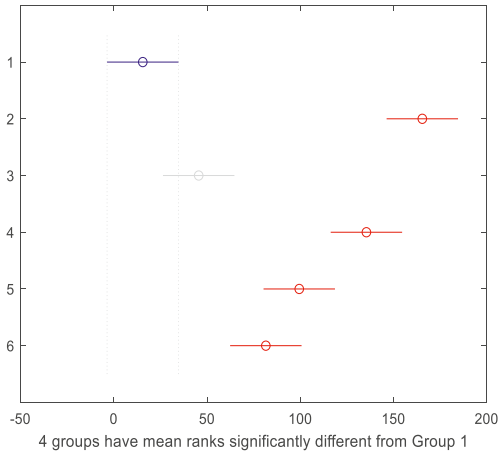

HCPSOSMA3

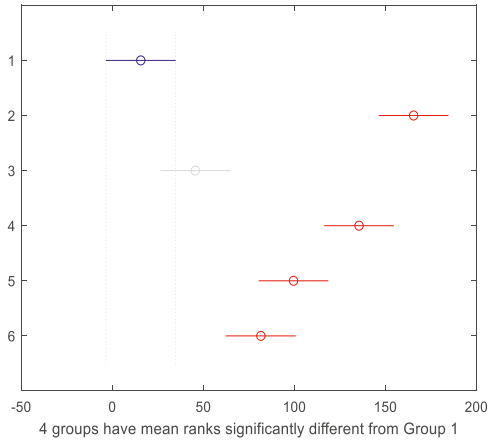

HCPSOSMA4

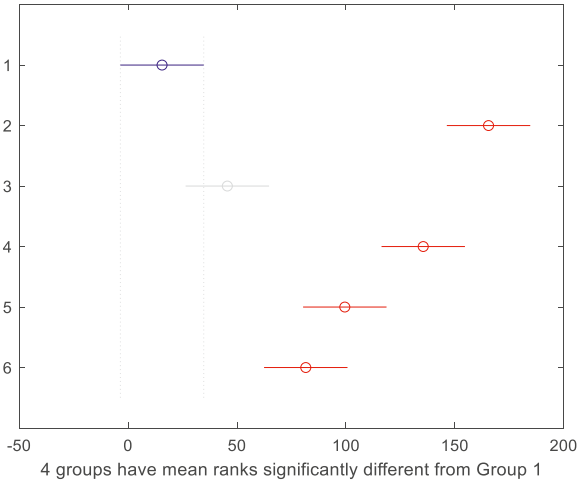

HCPSOSMA5

Fig. 14. Mean Ranking Multiple Comparisons using Kruskal-Wallis Test.

response to initial circumstances. The behavior of the nonlinear system will alter dramatically if the initial values differ slightly. Furthermore, a chaotic system possesses dynamic properties such as certainty, unpredictability, and sensitivity to initial circumstances, as well as a good internal structure. Based on these features, population variety can be preserved, avoiding the need for a local optimal search and enhancing the likelihood of a global optimum search.

As a dynamical system, chaos theory may be described by the following Equation:

$$cp_{k+1}^{i} = f\left(cp_{k}^{i}\right), i = 1, 2, 3 \ldots n \tag{28}$$

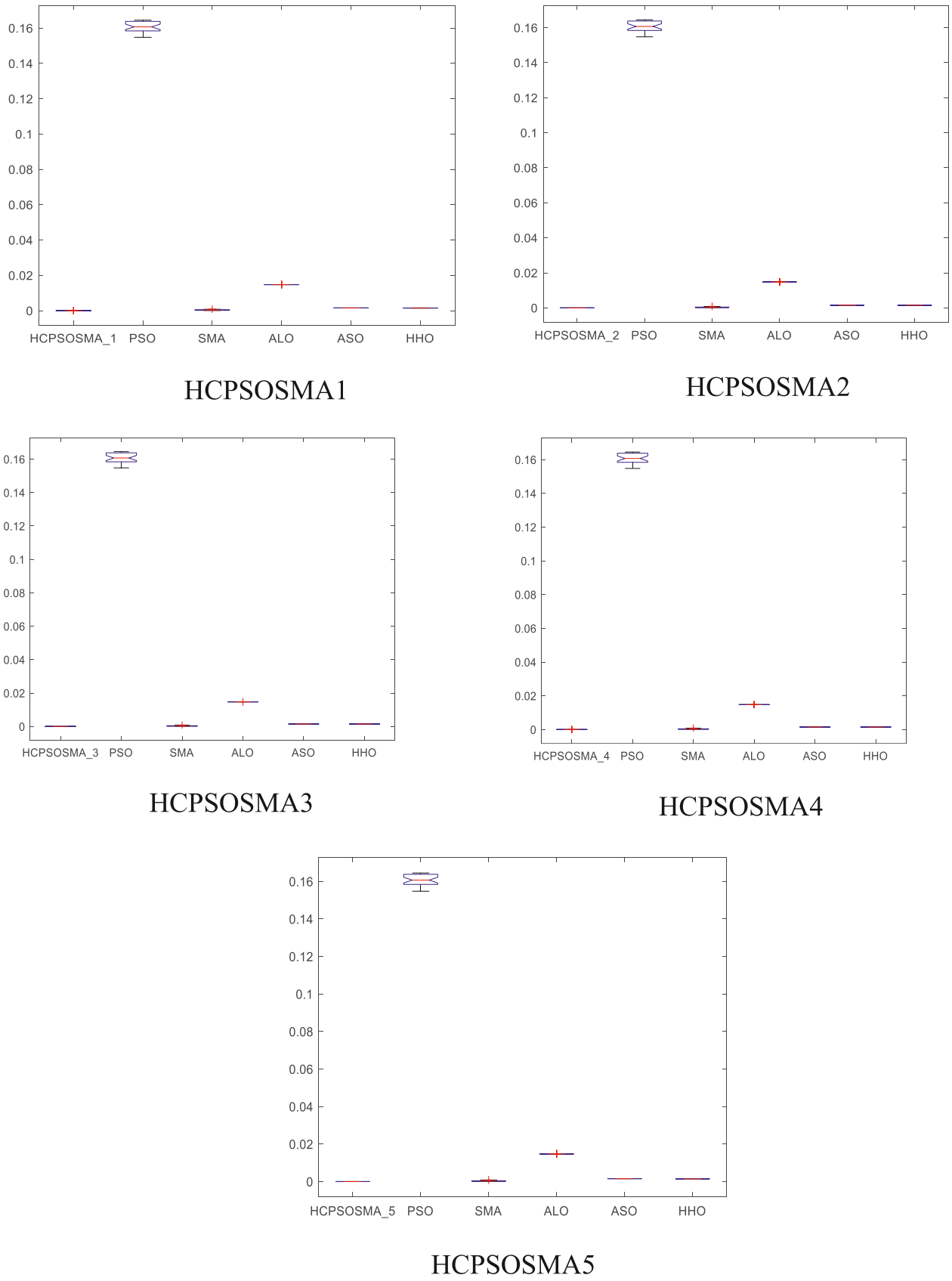

Fig. 15. Median Ranking Multiple Comparisons using Kruskal-Wallis Test.

Table 17
Mood's Median Test for Solar PV model.

SOURCE	SS	DF	MS	Chi-sq	Prob > Chi-sq	Algorithm
Columns	463824.1	5	92764.8	170.94	4.5965E-25	HCPSOSMA1
Error	21868.4	174	125.7	–	–	
Total	485692.5	179	–	–	–	
Columns	463824.1	5	92764.8	170.94	4.5955E-25	HCPSOSMA2
Error	21867.4	174	125.7	–	–	
Total	485691.5	179	–	–	–	
Columns	463824.1	5	92764.8	170.94	4.5945E-25	HCPSOSMA3
Error	21866.4	174	125.7	–	–	
Total	485690.5	179	–	–	–	
Columns	463824.1	5	92764.8	170.94	4.5985E-25	HCPSOSMA4
Error	21870.4	174	125.7	–	–	
Total	485694.5	179	–	–	–	
Columns	463824.1	5	92764.8	170.94	4.5975E-25	HCPSOSMA5
Error	21869.4	174	125.7	–	–	
Total	485693.5	179	–	–	–	

where 'n' refers to the map dimension. $f(cp_k^i)$ is a function that creates a chaotic model. There are several types of these maps that are utilized in various works of literature which are represented in Table 2 [66].

3.2. Hybrid chaotic particle swarm optimization slime mould algorithm (HCPSOSMA) technique

It has been shown that chaotic maps offer a number of benefits to the meta-heuristic method, and this can be seen in work done over the years [67]. The advantages of chaotic maps are investigated in this article as a possible component of a hybrid algorithm that we propose. Because the PSO algorithm is the parental algorithm for the swarm group of optimization algorithms, it enables the SMA algorithm to achieve a higher level of precision in its results. The challenge of employing chaotic maps to find the local minimum is solved by the hybrid chaotic algorithm that is described in this paper. The position of the chick in SMA is referred as variable "z" and is varied using chaotic maps. In addition, the accuracy of the system is improved by this approach. Pseudo code and flowchart of HCPSOSMA are shown in Figs. 4 and 5, respectively. The Table 3 represents the algorithm parameters and values used in the manuscript.

4. Results and discussions

4.1. Benchmark test function

Here, the proposed algorithm was evaluated by using a benchmark testing approach for parameter identification. A total of ten benchmarks are shown in Table 4, with one to seven functions being uni-modals and the remaining functions being multi-modals. In order to evaluate the performance and accuracy of the proposed algorithm, we compare it with some well-known meta-heuristic algorithms, including PSO, ASO, ALO, HHO, and SMA. A statistical analysis of the benchmark test functions is presented in Table 5. On the basis of Table 5, it can be concluded that the proposed algorithm has the lowest mean and standard deviation (SD) values compared with the other algorithms. This benchmark test function concludes that the proposed algorithm is more accurate, and has a better performance than the other algorithms that were compared.

4.2. Parameter estimation of the PEM fuel cell

In this section, the challenges associated with extracting parameters from the PEMFC model are solved through HCPSOSMA. The search range for the PEMFC model parameters is presented in Table 6. The PEMFC model parameter estimate datasheet is available for viewing in Table 7. In order to determine how effectively HCPSOSMA performs, a number of well-known meta-heuristics methods are tested and reviewed.

In this manuscript, the Ballard Mark-V system from the Canadian company Ballard [68,69] is employed to estimate the unknown parameters. The Ballard fuel cell stack system is made up of 35 individual cells that are stacked in sequence. Each cell in the system is made up of a Nafion 117 membrane and graphite electrodes embedded with a platinum catalyst in its Membrane Electrode Assembly, which has a total active cell area of 50.6 cm^2 with a membrane thickness of 178 μm. The reactant gases, such as pressurized hydrogen and air, are supplied from external tanks and humidified within the system by a humidifier. An air compressor delivers pressurized and cleaned dry air into the stack via a humidifier. While the partial pressure of hydrogen and oxygen is maintained a 1 bar. Furthermore, the PEMFC stack is kept at 343.15° Kelvin at all times, regardless of temperature changes. PEMFC parameter evaluation results along with computational time is shown in Table 8. The statistical findings of the Ballard Mark V are presented in Table 9. It is clear from this table that the recommended approach has the lowest average and standard deviation of all the methods considered.

The convergence curve for the Ballard Mark V model may be seen in Fig. 6. This graph makes it very evident that the approach that was offered is superior to all of the other algorithms that were compared. Once the parameters of the PEMFC have been evaluated, the I–V and P–I curves may then be computed. The characteristics of the V–I and P–I polarization curves are depicted in Figs. 7 and 8, respectively. Verifying that the measured outcomes using the provided algorithm model correspond to the experimental results is crucial here.

The outcomes of the Friedman ranking non-parametric test are presented in Table 10. In this testing, the HCPSOSMA variant family has a performance that is noticeably superior to that of the competing meta-heuristic techniques. In this examination, members of the HCPSOSMA variation family have achieved rankings one through five; SMA has achieved rank six, and PSO, ASO, ALO, and HHO are set to follow in their footsteps. In this study, the Wilcoxon rank-sum test serves as the second non-parametric analysis that is carried out. This test is widespread in dynamic programming and seems to be a straightforward, stable, and reliable non-parametric method for combined statistical analysis when samples are consistent [70]. The rank-sum test developed by Wilcoxon is utilized here, in addition to an HCPSOSMA variant family of additional algorithms. According to the results of this testing, the effectiveness of the HCPSOSMA variant family exceeds the other examined strategies, with a level of significance that corresponds to a probability range of 95%. The Kruskal-Wallis test is the third non-parametric test that was carried out for the purposes of this article [71–73]. Fig. 9 presents the results of a repeated comparison of mean rankings. When compared to the other groups, the HCPSOSMA variation family means rank is significantly different and significantly better. Fig. 10 presents the results of a repeated comparison of the median ranking. The HCPSOSMA variation family's median rank is significantly different from that of the other groups, and it is significantly higher. The

findings of the Mood's Median test are presented in Table 11. The importance of the probability is evaluated with the use of the chi-square test. According to the findings of the aforementioned non-parametric tests, it is possible to conclude that the approach that was recommended, the HCPSOSMA variant family, performed better than the other algorithms in terms of both reliability and speed.

4.3. Parameter estimation of the solar PV cell

In this section, HCPSOSMA solves parameter extraction problems for the solar PV model. The parameter search range of solar PV model is depicted in Table 12, and the datasheet for the solar model is shown in Table 13. Table 14 concluded that the best RMSE in comparison to other algorithms is the hybrid chaotic maps of HCPSOSMA and also shows the wilcoxon's rank sum test and computational time. Table 15 shows the statistical results of the solar PV model at STC. From this table also, it is concluded that the hybrid chaotic family has better performance in comparison to other algorithms. To study the efficiency of the HCPSOSMA computation, Fig. 10 shows the best convergence curves of the solar PV model acquired by PSO, SMA, ALO, ASO, HHO, HCPSOSMA1, HCPSOSMA2, HCPSOSMA3, HCPSOSMA4, and HCPSOSMA5. The convergence curves simply illustrate that HCPSOSMA has a faster rate of convergence than the other algorithms in the comparison. Fig. 11 represents the convergence graph of Solar PV model. This graph demonstrates quite clearly that the recommended method performs far better than the other algorithms that were compared. Following the completion of the parameter estimation for the Solar PV model, the I–V and P–I curves are derived. The parameters of the polarization curve of V–I and P–I are depicted in Figs. 12 and 13, respectively. In this scenario, it is important to confirm that the outputs that were assessed using the provided algorithm model are comparable to the values that were obtained from the experiments.

The outcomes of the Friedman ranking non-parametric test are presented in Table 16. In this test, the performance of the HCPSOSMA family is noticeably superior to that of the other meta-heuristic algorithms that were tested. In this testing, members of the HCPSOSMA family have achieved rankings one through five; SMA has achieved rank six, and PSO, ASO, ALO, and HHO will follow in their footsteps. In this research, the Wilcoxon rank-sum test serves as the second non-parametric analysis that is carried out. This test is widespread in dynamic programming and appears to be a straightforward, stable, and reliable non-parametric method for combined statistical analysis when samples are consistent. The rank-sum test developed by Wilcoxon is utilized here, in addition to a family of additional algorithms known as HCPSOSMA. According to the results of this testing, the effectiveness of the HCPSOSMA variant family exceeds the remaining of the analyzed techniques, with a level of significant that corresponds to a probability range of 95%. The Kruskal-Wallis test is the third non-parametric test that was carried out for the purposes of this article. Fig. 14 presents the results of the numerous comparisons of mean ranking. When compared to the other groups, the HCPSOSMA variation family means rank is significantly different and significantly better. Fig. 15 presents the results of a repeated comparison of the median ranking. The HCPSOSMA variation family's median rank is significantly different from that of the other groups, and it is significantly higher. The outcomes of the Mood's Median test are presented in Table 17. The importance of the probability is evaluated with the help of the chi-square test. According to the findings of the aforementioned non-parametric tests, it is possible to draw the conclusion that the approach that was recommended, the HCPSOSMA variant family, performed better than the other algorithms in terms of reliability and accuracy.

5. Conclusions

This paper presents a stochastic novel metaheuristic technique for evaluating the parameters of a hybrid system (PEMFC and TDM). In order to optimize the solution vector parameters and achieve high effectiveness, the recommended family of hybrid chaotic variations is built with adaptive weight. This was done to maximize the advantages of the hybrid chaotic variations. The family of hybrid chaotic variants is applied to the hybrid system to test its reliability and performance. The following are some of the conclusions that can be derived from the test results:

- The results proved that proposed algorithm has overcome the PSO tendency to struck in local minima and to solve the complex mathematical problem with ease
- In terms of precision and convergence speed of global optimization problems, the family of hybrid chaotic versions outperforms the other comparison strategies tested in the research.
- According to the statistical findings, the family of hybrid chaotic variants is now more effective at extracting parameters from hybrid systems.
- The sum of square error results come out to be 3.78E-16 for the HCPSOSMA2 and remaining algorithms follow them for the PEMFC.
- The root mean square error results come out to be 4.31E-13 for the HCPSOSMA3 and remaining algorithms follow them for the TDM.
- When compared to other comparable methods, the family of hybrid chaotic variants shows better or equivalent efficiency on hybrid systems, as shown by the results of the solution consistency test, the I–V and P–V characteristic curves, the Friedman ranking test, the Wilcoxon's rank sum test, and the Kruskal-Wallis test.

References

[1] Hille E, Althammer W, Diederich H. Environmental regulation and innovation in renewable energy technologies: does the policy instrument matter? Technol Forecast Soc Change 2020;153:119921.
[2] Al-Badi A, Al Wahaibi A, Ahshan R, Malik A. Techno-economic feasibility of a solar-wind-fuel cell energy system in duqm, Oman. Energies 2022;15:5379.
[3] Yakout AH, Hasanien HM, Kotb H. Proton exchange membrane fuel cell steady state modeling using marine predator algorithm optimizer. Ain Shams Eng J 2021;12:3765–74.
[4] Li D, Ma Z, Shao W, Li Y, Guo X. Finite time thermodynamic modeling and performance analysis of high-temperature proton exchange membrane fuel cells. Int J Mol Sci 2022;23:9157.
[5] Mohamed MA, Mirjalili S, Dampage U, Salmen SH, Obaid SA, Annuk A. A cost-efficient-based cooperative allocation of mining devices and renewable resources enhancing blockchain architecture. Sustainability 2021;13:10382.
[6] Hejri M, Mokhtari H. On the comprehensive parametrization of the photovoltaic (PV) cells and modules. IEEE J. Photovolt. 2017;7:250–8.
[7] Oliva D, Cuevas E, Pajares G. Parameter identification of solar cells using artificial bee Colony optimization. Energy (Oxf.) 2014;72:93–102.
[8] Jordehi AR. Parameter estimation of solar photovoltaic (PV) cells: a review. Renew Sustain Energy Rev 2016;61:354–71.
[9] Chandran BP, Selvakumar AI, Mathew FM. Integrating multilevel converters application on renewable energy sources—a survey. J Renew Sustain Energy 2018;10:065502.
[10] El-Fergany AA. Electrical characterisation of proton exchange membrane fuel cells stack using grasshopper optimiser. IET Renew Power Gener 2018;12:9–17.
[11] El-Fergany AA. Extracting optimal parameters of PEM fuel cells using Salp swarm optimizer. Renew Energy 2018;119:641–8.
[12] Fathy A, Rezk H. Multi-verse optimizer for identifying the optimal parameters of PEMFC model. Energy (Oxf.) 2018;143:634–44.
[13] Ali M, El-Hameed MA, Farahat MA. Effective parameters' identification for polymer electrolyte membrane fuel cell models using Grey Wolf optimizer. Renew Energy 2017;111:455–62.
[14] Askarzadeh A, Coelho L. A backtracking 486 search algorithm combined with burger's chaotic map for parameter estimation of PEMFC electrochemical model. Int J Hydrogen Energy 2014;39:11165–74.
[15] Turgut OE, coban MT. Optimal proton exchange membrane fuel cell modeling based on hybrid teaching learning based optimization-differential evolution algorithm. Ain Shams Eng J 2016;7:347–60.
[16] Askarzadeh A, Rezazadeh A. An innovative global Harmony search algorithm for parameter identification of a PEM fuel cell model. IEEE Trans Ind Electron 2012;59:3473–80.
[17] Jiang B, Wang N, Wang L. Parameter identification for solid oxide fuel cells using cooperative barebone particle swarm optimization with hybrid learning. Int J Hydrogen Energy 2014;39:532–42.
[18] Oliva D, Elaziz MA, Elsheikh AH, Ewees AA. A review on meta-heuristics methods for estimating parameters of solar cells. J Power Sources 2019;435:126683.

[19] Saadaoui D, Elyaqouti M, Assalaou K, Ben hmamou D, Lidaighbi S. Parameters optimization of solar PV cell/module using genetic algorithm based on non-uniform mutation. Energy Convers Manag X 2021;12:100129.
[20] Jordehi AR. Enhanced leader particle swarm optimisation (ELPSO): an efficient algorithm for parameter estimation of photovoltaic (PV) cells and modules. Sol Energy 2018;159:78–87.
[21] Nunes HGG, Pomboa JAN, Marianoa SJPS, caladoa MRA, Felippe de Souza JAM. A new high performance method for determining the parameters of PV cells and modules based on guaranteed convergence particle swarm optimization. Appl Energy 2018;211:774–91.
[22] Qin HX, Han YY, Zhang B, Meng LL, Liu YP, Pan QK, Gong DW. An improved iterated greedy algorithm for the energy-efficient blocking hybrid flow shop scheduling problem. Swarm Evol Comput 2022;69:100992.
[23] Han X, Han Y, Zhang B, Qin H, Li J, Liu Y, Gong D. An effective iterative greedy algorithm for distributed blocking flowshop scheduling problem with balanced energy costs criterion. Appl Soft Comput 2022;129:109502.
[24] Mahato DP, Sandhu JK, Singh NP, Kaushal V. On scheduling transaction in grid computing using cuckoo search-ant colony optimization considering load, vol. 23. Cluster Computing; 2020. p. 1483–504.
[25] Rani S, Babbar H, Kaur P, Alshehri MD, Shah SHA. An optimized approach of dynamic target nodes in wireless sensor network using bio inspired algorithms for maritime rescue. IEEE Trans Intell Transport Syst 2022.
[26] Oliva D, Ewees AA, Aziz MAE, Hassanien AE, Peréz-Cisneros MA. Chaotic improved artificial bee Colony for parameter estimation of photovoltaic cells. Energies 2017;10:865.
[27] Chen X, Xu B, Mei C, Ding Y, Li K. Teaching–learning–based artificial bee Colony for solar photovoltaic parameter estimation. Appl Energy 2018;212:1578–88.
[28] Rajasekar N, Krishna Kumar N, Venugopalan R. Bacterial foraging algorithm based solar PV parameter estimation. Sol Energy 2013;97:255–65.
[29] Subudhi B, Pradhan R. Bacterial foraging 618 optimization approach to parameter extraction of a photovoltaic module. IEEE Trans Sustain Energy 2017;9:381–9.
[30] Mokeddem D. Parameter extraction of solar photovoltaic models using enhanced Levy Flight based grasshopper optimization algorithm. J. Electr. Eng. Technol. 2021;16:171–9.
[31] Alam DF, Yousri DA, Eteiba MB. Flower pollination algorithm based solar PV parameter estimation. Energy Convers Manag 2015;101:410–22.
[32] Xu S, Wang Y. Parameter estimation of photovoltaic modules using a hybrid flower pollination algorithm. Energy Convers Manag 2017;144:53–68.
[33] Yu K, Liang JJ, Qu BY, Chen X, Wang H. Parameters identification of photovoltaic models using an improved JAYA optimization algorithm. Energy Convers Manag 2017;150:742–53.
[34] Yu K, Qu B, Yue C, Ge S, Chen X, Liang J. A performance-guided JAYA algorithm for parameters identification of photovoltaic cell and module. Appl Energy 2019; 237:241–57.
[35] Xiong G, Zhang J, Shi D, Zhu L, Yuan X. Parameter extraction of solar photovoltaic models with an either-or teaching learning based algorithm. Energy Convers Manag 2020;224:113395.
[36] Askarzadeh A, dos Santos Coelho L. Determination of photovoltaic modules parameters at different operating conditions using a novel Bird mating optimizer approach. Energy Convers Manag 2015;89:608–14.
[37] Patel SJ, Panchal AK, Kheraj V. Extraction of 591 solar cell parameters from a single current-voltage characteristic using teaching learning based optimization algorithm. Appl Energy 2014;119:384–93.
[38] Yu K, Chen X, Wang X, Wang Z. Parameters identification of photovoltaic models using self-adaptive teaching-learning-based optimization. Energy Convers Manag 2017;145:233–46.
[39] Chen Z, Wu L, Lin P, Wu Y, Cheng S. Parameters identification of photovoltaic models using hybrid adaptive Nelder-Mead Simplex algorithm based on Eagle strategy. Appl Energy 2016;182:47–57.
[40] Hassan KH, Rashid AT, Jasim BH. Parameters estimation of solar photovoltaic module using Camel behavior search algorithm. Int J Electr Comput Eng (IJECE) 2021;11:788.
[41] Wang S, Yu Y, Hu W. Static and dynamic solar photovoltaic models' parameters estimation using hybrid rao optimization algorithm. J Clean Prod 2021;315: 128080.
[42] Premkumar M, Sowmya R, Jangir P, Siva Kumar JSV. A new and reliable objective functions for extracting the unknown parameters of solar photovoltaic cell using political optimizer algorithm. In: Proceedings of the 2020 international conference on data analytics for business and industry: way towards a sustainable economy (ICDABI); 2020. IEEE.
[43] Ahmed WAEM, Mageed HMA, Mohamed SA, Saleh AA. Fractional order darwinian particle swarm optimization for parameters identification of solar PV cells and modules. Alex Eng J 2022;61:1249–63.
[44] Wang J, Yang B, Li D, Zeng C, Chen Y, Guo Z, Zhang X, Tan T, Shu H, Yu T. Photovoltaic cell parameter estimation based on improved Equilibrium optimizer algorithm. Energy Convers Manag 2021;236:114051.
[45] Lin H, Ahmadianfar I, Amiri Golilarz N, Jamei M, Heidari AA, Kuang F, Zhang S, Chen H. Adaptive slime mould algorithm for optimal design of photovoltaic models. Energy Sci Eng 2022;10:2035–64.
[46] Fathy A, Rezk H. Parameter estimation of photovoltaic system using imperialist competitive algorithm. Renew Energy 2017;111:307–20.
[47] Askarzadeh A, Rezazadeh A. Parameter identification for solar cell models using Harmony search-based algorithms. Sol Energy 2012;86:3241–9.
[48] Beigi AM, Maroosi A. Parameter identification for solar cells and module using a hybrid firefly and pattern search algorithms. Sol Energy 2018;171:435–46.
[49] Premkumar M, Jangir P, Ramakrishnan C, Nalinipriya G, Alhelou HH, Kumar BS. Identification of solar photovoltaic model parameters using an improved gradient-based optimization algorithm with chaotic drifts. IEEE Access 2021;9:62347–79.
[50] Allam D, Yousri DA, Eteiba MB. Parameters extraction of the three diode model for the multi-crystalline solar cell/module using moth-flame optimization algorithm. Energy Convers Manag 2016;123:535–48.
[51] Kler D, Sharma P, Banerjee A, Rana KPS, Kumar V. PV cell and module efficient parameters estimation using evaporation rate based water cycle algorithm. Swarm Evol Comput 2017;35:93–110.
[52] Rezk H, Fathy A. A novel optimal parameters identification of triple-junction solar cell based on a recently meta-heuristic water cycle algorithm. Sol Energy 2017; 157:778–91.
[53] Hasanien HM. Shuffled Frog leaping algorithm for photovoltaic model identification. IEEE Trans Sustain Energy 2015;6:509–15.
[54] Premkumar M, Babu TS, Umashankar S, Sowmya R. A new metaphor-less algorithms for the photovoltaic cell parameter estimation. Optik 2020;208:164559.
[55] Stein NE, Hamelers HMV, van Straten G, Keesman KJ. On-line detection of toxic components using a microbial fuel cell-based biosensor. J Process Control 2012;22: 1755–61.
[56] Jain A. Exact analytical solutions of the parameters of real solar cells using Lambert W-function. Sol Energy Mater Sol Cells 2004;81:269–77.
[57] Humada AM, Hojabri M, Mekhilef S, Hamada HM. Solar cell parameters extraction based on single and double-diode models: a review. Renew Sustain Energy Rev 2016;56:494–509.
[58] Kashefi H, Sadegheih A, Mostafaeipour A, Mohammadpour Omran M. Parameter identification of solar cells and fuel cell using improved social spider algorithm. COMPEL-The international journal for computation and mathematics in electrical and electronic engineering 2021;40(2):142–72.
[59] Niu Q, Zhang L, Li K. A biogeography-based optimization algorithm with mutation strategies for model parameter estimation of solar and fuel cells. Energy Convers Manag 2014;86:1173–85.
[60] Niu Q, Zhang H, Li K. An improved TLBO with elite strategy for parameters identification of PEM fuel cell and solar cell models. Int J Hydrogen Energy 2014; 39(8):3837–54.
[61] Singla MK, Oberoi AS, Nijhawan P. Solar-PV & fuel cell based hybrid power solution for remote locations. Int J Eng Adv Technol 2019;9:861–7.
[62] Singla MK, Nijhawan P, Oberoi AS. Hydrogen fuel and fuel cell Technology for cleaner future: a review. Environ Sci Pollut Res Int 2021;28:15607–26.
[63] Howard FL. The life history of physarumpolycephalum. Am J Bot 1931:116–33.
[64] Camp WG. A method of cultivating myxomycete plasmodia. Bull Torrey Bot Club 1936;63:205.
[65] Örnek BN, Aydemir SB, Düzenli T, Özak B. A novel version of slime mould algorithm for global optimization and real world engineering problems. Math Comput Simulat 2022;198:253–88.
[66] Elazab OS, Hasanien HM, Elgendy MA, abdeen AM. Parameters estimation of single-and multiple-diode photovoltaic model using whale optimisation algorithm. IET Renew Power Gener 2018;12:1755–61.
[67] Singla MK, Nijhawan P, Oberoi AS. A novel hybrid particle swarm optimization rat search algorithm for parameter estimation of solar PV and fuel cell model. COMPEL-The international journal for computation and mathematics in electrical and electronic engineering 2022.
[68] Correa JM, Farret FA, Canha LN. Proceeedings of 27th annual conference of the IEEE industrial electronics society. 2001. p. 141–6.
[69] Al-Fayoumi M, Al-Haija QA, Armoush R, Amareen C. XAI-PDF: a robust framework for malicious PDF detection leveraging SHAP-based feature engineering. Int. Arab J. Inf. Technol. 2024;21(1):128–46.
[70] Singla MK, Nijhawan P, Oberoi AS. Parameter estimation of proton exchange membrane fuel cell using a novel meta-heuristic algorithm. Environ Sci Pollut Control Ser 2021;28(26):34511–26.
[71] Gupta J, Nijhawan P, Ganguli S. Parameter estimation of different solar cells using a novel swarm intelligence technique. Soft Comput 2022;26(12):5833–63.
[72] Mahato DP, Sandhu JK, Singh NP, Kaushal V. On scheduling transaction in grid computing using cuckoo search-ant colony optimization considering load, vol. 23. Cluster Computing; 2020. p. 1483–504.
[73] Rani S, Babbar H, Kaur P, Alshehri MD, Shah SHA. An optimized approach of dynamic target nodes in wireless sensor network using bio inspired algorithms for maritime rescue. IEEE Trans Intell Transport Syst 2022.